

Accepted Manuscript

Asymmetrical *meta*-methoxylated diarylpentanoids: Rational design, synthesis and anti-cancer evaluation *in-vitro*

Sze Wei Leong, Suet Lin Chia, Faridah Abas, Khatijah Yusoff



PII: S0223-5234(18)30710-4

DOI: [10.1016/j.ejmech.2018.08.039](https://doi.org/10.1016/j.ejmech.2018.08.039)

Reference: EJMECH 10650

To appear in: *European Journal of Medicinal Chemistry*

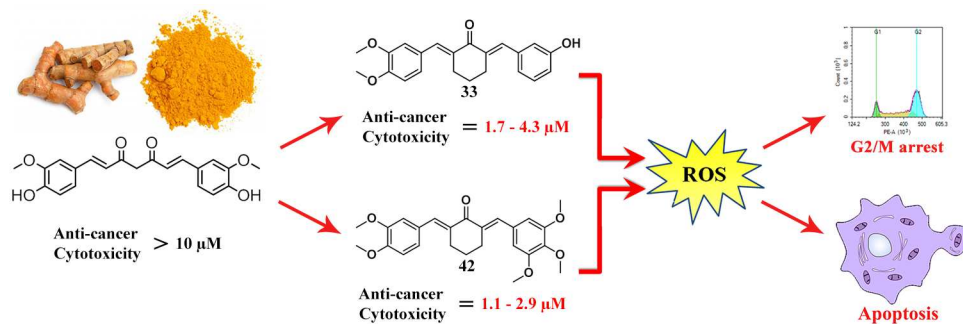
Received Date: 14 November 2017

Revised Date: 11 August 2018

Accepted Date: 14 August 2018

Please cite this article as: S.W. Leong, S.L. Chia, F. Abas, K. Yusoff, Asymmetrical *meta*-methoxylated diarylpentanoids: Rational design, synthesis and anti-cancer evaluation *in-vitro*, *European Journal of Medicinal Chemistry* (2018), doi: 10.1016/j.ejmech.2018.08.039.

This is a PDF file of an unedited manuscript that has been accepted for publication. As a service to our customers we are providing this early version of the manuscript. The manuscript will undergo copyediting, typesetting, and review of the resulting proof before it is published in its final form. Please note that during the production process errors may be discovered which could affect the content, and all legal disclaimers that apply to the journal pertain.



Asymmetrical *meta*-methoxylated diarylpentanoids: Rational design, synthesis and anti-cancer evaluation *in-vitro*

Sze Wei Leong ^{a*}, Suet Lin Chia ^{a,b}, Faridah Abas ^{b,c}, Khatijah Yusoff ^{a,d*}

^a*Department of Microbiology, Faculty of Biotechnology and Biomolecular Sciences, Universiti Putra Malaysia, 43400 UPM, Serdang, Selangor Darul Ehsan, Malaysia*

^b*Institute of Bioscience, Universiti Putra Malaysia, 43400 UPM, Serdang, Selangor Darul Ehsan, Malaysia*

^c*Department of Food Science, Faculty of Food Science and Technology, Universiti Putra Malaysia, 43400 UPM, Serdang, Selangor, Malaysia.*

^d*Malaysia Genome Institute (MGI), National Institute of Biotechnology Malaysia (NIBM), Jalan Bangi, 43000 Kajang, Selangor Darul Ehsan, Malaysia.*

*Corresponding authors

Tel +603-89467765; Fax: +603-89467590

E-mail address: leongszewei@upm.edu.my (SW. Leong), kyusoff@upm.edu.my (K. Yusoff)

Abstract

In the present study, a series of forty-five asymmetrical *meta*-methoxylated diarylpentanoids have been synthesized, characterized and evaluated for their *in-vitro* anti-cancer potential. Among the forty-five analogs, three compounds (**20**, **33** and **42**) have been identified as lead compounds due to their excellent inhibition against five human cancer cell lines including SW620, A549, EJ28, HT1080 and MCF-7. Structure-activity relationship study on cytotoxicity of tested compounds suggested that the presence of *meta*-oxygenated phenyl ring played a critical role in enhancing their cytotoxic effects. Compounds **33** and **42** in particular, exhibited strongest cytotoxicity against tested cell lines with the IC₅₀ values ranging from 1.1 to 4.3 μ M. Subsequent colony formation assay on SW620 cell line showed that both compounds **33** and **42** possessed strong anti-proliferative activity. In addition, flow cytometry based experiments revealed that these compounds could trigger intracellular ROS production thus inducing G2/M-phase cell arrest and apoptosis. All these results suggested that poly *meta*-oxygenated diarylpentnoid is a promising scaffold which deserved further modification and investigation in the development of natural product-based anti-cancer drug.

Keywords:

Assymetrical diarylpentanoids; Cytotoxicity; Anti-proliferative; Cell cycle; Apoptosis; Intracellular ROS

1. Introduction

Cancer is one of the leading causes of morbidity and mortality worldwide, with approximately 14 million new cases in 2012. Worryingly, this number is estimated to rise by about 70% over the next two decades. According to the global cancer database (Globocan) in 2012, there are 32.6 million people who were diagnosed with cancer and the number of cancer-related deaths has exceeded 8.2 million cases [1]. This disquieting situation is worsening by its effect on global economy as cancer has badly hit the economy with an estimated cost of 1.16 trillion USD in 2010 [2]. Thus, considering the global human and economic health, safer cancer therapies with better effectiveness are currently being pursued.

To date, cancer treatments are mostly relying on chemotherapy especially for late-stage or complex cancers. Paclitaxel, cisplatin, and docetaxel are considered as the most prominent chemodrugs due to their excellent killing effects on various cancer cell lines including breast, head and neck, prostate and lung cancer cells. Paclitaxel and docetaxel belong to the taxane family that function by stabilizing the microtubules thus thwarting cell mitosis while cisplatin is a platinum-based compound that prevents cell mitosis by cross-linking DNA [3-6]. Unfortunately, the full potential of these drugs is far from being realized due to their associated severe side effects such as extreme fatigue and leukopenia, which are caused by their low selectivity towards cancer cells [7]. These unpleasant side effects not only reduce the life quality of cancer patients, but may also threaten their survival. Thus, finding safer drugs with improved selectivity has been the focus of current anticancer drug discovery.

Curcumin is a naturally occurring small molecule which is well-known for its medicinal potential. Curcumin has been proven to exhibit remarkable antioxidant, anti-inflammatory and anticancer properties

upon its strong superoxides and free radicals inhibition, pro-inflammatory cytokines and enzymes suppression, and cancer cells apoptosis induction [8-12]. Together with its excellent safety profile and extremely mild side effects, curcumin has been suggested to be the most potent candidate in the discovery of alternative cancer therapeutic agents. However, the practical use of curcumin is derogated by its low bioavailability due to its poor absorbability and stability which caused by the presence of unstable β -diketone moiety [13]. Thus, structural optimization to remove the unstable β -diketone moiety of curcumin is an inevitable effort to reveal its full therapeutic potential by developing a derivative molecule with improved bioactivities and stability.

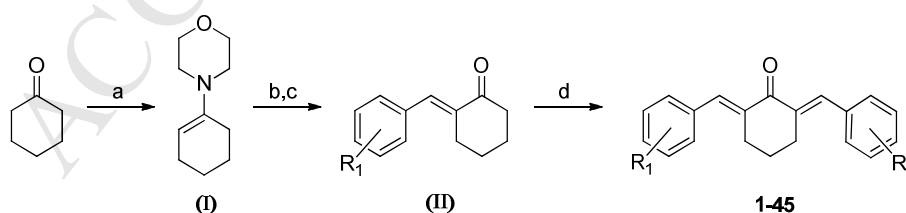
Diarylpentanoids, a 5-carbon spacer series formed by the synthetic modification of curcumin has gained increasing attention due to their superior enhanced medicinal properties, particularly as anticancer agents [14-17]. They have been shown to exhibit remarkable anticancer properties as they significantly inhibited the growth of various cancer cell lines including breast, lung, colon, pancreatic and prostate cancer cells, through their anti-proliferative and anti-angiogenic activities [18-22]. In addition, diarylpentanoids were also found to induce cancer cell apoptosis by simultaneously inhibiting and activating the Bcl-2 proteins and caspases, respectively [23-26]. Unlike curcumin, diarylpentanoids are chemically stable at physiological pH and metabolically stable in rat liver microsomes, which prompted them to be the most impactful candidates among the curcuminoids that deserve further intensive investigations with the goal of developing novel safer chemodrugs [23, 27].

Previous research found that vanillin and adjacent methoxyphenyl moieties on both terminals of diarylpentanoids are responsible for their apoptosis inducing ability [28-30]. However, our structure activity relationship (SAR) study suggests that *meta*-methoxyphenyl group could be the most crucial functional group due to its presence in majority of the reported structures. This idea is further supported by their structure similarity with several known anti-tubulin agents including colchicine and combretastatin A-4, as well as their anti-tubulin enhancing effects on reported diarylpentanoids [31, 32]. Surprisingly, several recent studies showed that the asymmetrical diarylpentanoids exhibited similar activity to their respective symmetrical analogs suggesting that only a single substitution on the diarylpentanoid scaffold is sufficient to prepare compounds active in inducing apoptosis [23, 26, 33]. On the basis of these observations, the aim of the present study is to develop a series of rare asymmetrical *meta*-methoxyphenyl-containing diarylpentanoids and evaluate for their oncolytic potential.

2. Results and Discussion

2.1 Chemistry

Scheme 1. General synthetic steps for compounds **1-45**^x

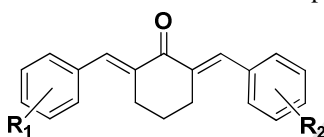


^xReagents and conditions: (a) morpholine, *p*-toluene-sulphonic acid, toluene, reflux (2h); (b) methoxylated benzaldehyde, 80°C (8h); (c) H₂O, reflux (0.5h); (d) benzaldehyde, EtOH, 10M NaOH, RT (overnight).

The synthesis of *meta*-methoxyphenyl-containing diarylpentanoids is outlined in **Scheme 1**. As shown in **Scheme 1**, compounds **1-45** were achieved through two different carbonyl-group addition reactions

namely Stork enamine alkylation and aldol condensation [34, 35]. Stork enamine alkylation was first carried out to prepare key intermediate **I** by reacting cyclohexanone with morpholine under reflux condition. In order to obtain maximum yield, Dean-Stark apparatus was employed to prevent hydrolysis of desired enamine by removing water by product. Enamine **I** formed was then reacted with 2,3- or 3,4-dimethoxybenzaldehyde to afford intermediate **II**. Upon purification, intermediate **II** was further reacted with appropriate benzaldehydes under base-catalyzed aldol condensation conditions to give target compounds **1-45**. The formation of the final product was confirmed by detection of two singlets at chemical shift of 7.5-8.0 ppm in the proton NMR spectra which represents the vinylic protons of bezylidenes. All synthesized compounds were purified by column chromatography and characterized by $^1\text{H-NMR}$, $^{13}\text{C-NMR}$, and high-resolution electron impact-mass spectrometry (HRMS). Prior to assays, the purity of synthesized compounds were confirmed to be greater than 95% based on their respective HPLC profiles. The synthesized compounds were listed in **Table 1**.

Table 1. Chemical structures of compounds **1-45**



Compound	R ₁	R ₂	Compound	R ₁	R ₂
1		2-Cl	24		2-Cl
2		3-Cl	25		3-Cl
3		4-Cl	26		4-Cl
4		2-Br	27		2-Br
5		3-Br	28		3-Br
6		4-Br	29		4-Br
7		2-OMe	30		2-OMe
8		3-OMe	31		3-OMe
9		4-OMe	32		4-OMe
10		3-OH	33		3-OH
11		4-OH	34		4-OH
12	2,3-OMe	2,3-Cl	35	3,4-OMe	2,3-Cl
13		2,4-Cl	36		2,4-Cl
14		3,4-Cl	37		3,4-Cl
15		3,5-Cl	38		3,5-Cl
16		2,3-OMe	39		2,4-OMe
17		2,4-OMe	40		3,4-OMe
18		3,4-OMe	41		3,5-OMe
19		3,5-OMe	42		3,4,5-OMe
20		3,4,5-OMe	43		3-Cl-4-OH
21		3-Cl-4-OH	44		4-OH-3-OMe
22		4-OH-3-OMe	45		3,4-OH
23		3,4-OH			

2.2 Biological Studies

2.2.1 In-vitro cytotoxic activity

The *in-vitro* cytotoxic activity of the synthesized compounds on five human cancer cell lines including SW620, A549, EJ28, HT1080 and MCF-7 were determined by MTT assay as previously described [36]. The preliminary screening results are summarized and compiled in **Figure 1**.

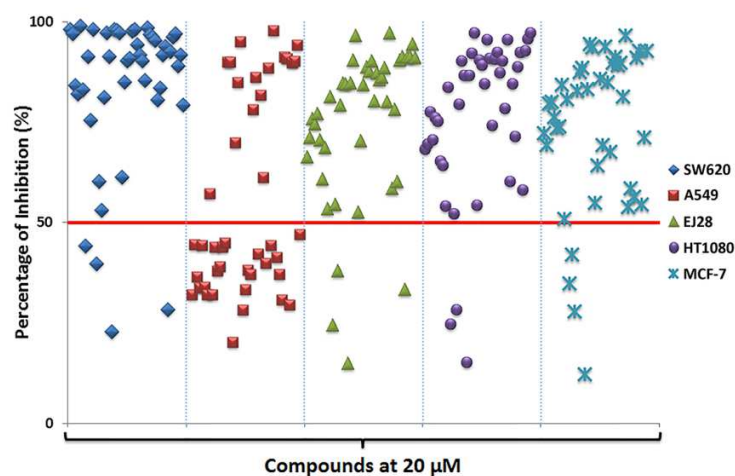
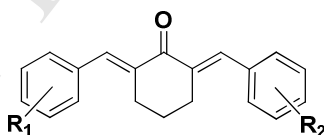


Figure 1. Inhibitory activities of synthesized compounds against various cancer cell lines at a testing concentration of 20 μM . The red line across the graph represents the threshold percentage for further IC_{50} determination

As depicted in **Figure 1**, all compounds displayed significant cytotoxic effect (above 50% inhibition) against all tested cancer cell lines at a testing concentration of 20 μM suggesting that *meta*-methoxyphenyl-containing diarylpentanoid is a promising anti-cancer scaffold. On the other hand, considering the inhibitory selectivity of synthesized compounds on different cancer cell lines, this diarylpentanoid system appeared to be a weaker A549 targeting structure as majority of the tested analogs showed lower A549 inhibition compared to their respective activity on other cell lines. In order to gain better insight into the role of different structural functionalities on cytotoxic effect, IC_{50} determination and SAR study were performed. The calculated cytotoxic IC_{50} values of the synthesized compounds on various cell lines are presented in **Table 2**, in which curcumin and normal human dermal fibroblasts (NHDF) were served as controls. Heatmap (**Figure 2**) was also generated using GraphPad Prism v7.0 (Graphpad Software, La Jolla, California, USA) to provide an overview on the IC_{50} performance of the synthesized compounds against the various cancer cells.

Table 2. Cytotoxicity of compounds 1-45 on SW620, A549, EJ28, HT1080, MCF-7 and NHDF cell lines.



Compound	R1	R2	IC_{50} (μM)					NHDF
			SW620	A549	EJ28	HT1080	MCF-7	
Curcumin	-	-	14.0	17.9	10.5	13.1	9.8	24.1
1	2,3-OMe	2-Cl	10.3	>20	12.0	11.7	11.3	44.2
2	2,3-OMe	3-Cl	9.1	>20	11.3	10.3	12.0	21.4
3	2,3-OMe	4-Cl	11.1	>20	11.0	11.1	10.3	18.6
4	2,3-OMe	2-Br	12.1	>20	10.8	10.8	9.7	>50
5	2,3-OMe	3-Br	8.8	>20	12.1	12.2	11.7	23.9
6	2,3-OMe	4-Br	11.1	>20	15.2	13.7	13.8	21.4
7	2,3-OMe	2-OMe	>20	>20	16.6	14.1	12.0	31.3
8	2,3-OMe	3-OMe	7.0	16.4	10.0	9.9	5.9	16.4
9	2,3-OMe	4-OMe	13.6	>20	16.8	16.3	18.6	43.5
10	2,3-OMe	3-OH	6.4	>20	8.5	8.5	8.8	19.3
11	2,3-OMe	4-OH	>20	>20	>20	>20	>20	>50
12	2,3-OMe	2,3-Cl	16.3	>20	18.1	19.3	>20	>50
13	2,3-OMe	2,4-Cl	16.3	>20	>20	>20	>20	49.2

14	2,3-OMe	3,4-Cl	10.0	>20	12.1	10.8	9.0	25.5
15	2,3-OMe	3,5-Cl	5.5	12.5	7.5	6.1	4.3	21.6
16	2,3-OMe	2,3-OMe	8.3	11.4	8.4	6.1	5.0	31.0
17	2,3-OMe	2,4-OMe	>20	>20	>20	>20	>20	>50
18	2,3-OMe	3,4-OMe	6.4	14.4	6.6	6.4	6.5	14.9
19	2,3-OMe	3,5-OMe	3.8	10.2	3.6	4.5	1.7	13.1
20	2,3-OMe	3,4,5-OMe	2.5	5.9	2.4	2.3	1.4	7.9
21	2,3-OMe	3-Cl-4-OH	16.8	>20	18.3	14.3	16.4	39.5
22	2,3-OMe	4-OH-3-OMe	8.6	>20	10.6	5.9	11.6	14.3
23	2,3-OMe	3,4-OH	6.3	>20	6.4	4.7	4.7	17.9
24	3,4-OMe	2-Cl	7.1	>20	6.9	6.8	10.4	21.6
25	3,4-OMe	3-Cl	5.1	11.0	5.4	4.9	6.0	11.9
26	3,4-OMe	4-Cl	5.9	10.1	5.7	4.8	6.3	11.2
27	3,4-OMe	2-Br	5.3	>20	7.4	8.4	9.5	21.8
28	3,4-OMe	3-Br	4.2	12.8	4.9	5.2	5.3	12.4
29	3,4-OMe	4-Br	5.2	16.0	7.1	4.3	6.9	13.1
30	3,4-OMe	2-OMe	7.8	>20	8.1	8.1	8.0	18.1
31	3,4-OMe	3-OMe	3.7	6.7	4.2	4.6	4.6	11.6
32	3,4-OMe	4-OMe	6.6	>20	8.4	7.2	7.8	30.9
33	3,4-OMe	3-OH	1.9	4.3	1.8	1.7	2.9	6.8
34	3,4-OMe	4-OH	7.7	>20	16.6	16.8	17.0	26.1
35	3,4-OMe	2,3-Cl	10.8	>20	10.4	8.8	14.3	18.5
36	3,4-OMe	2,4-Cl	10.3	>20	12.4	10.5	16.2	>50
37	3,4-OMe	3,4-Cl	4.0	6.9	3.4	3.1	4.4	10.1
38	3,4-OMe	3,5-Cl	2.5	5.5	4.2	3.0	3.8	8.3
39	3,4-OMe	2,4-OMe	>20	>20	>20	17.1	15.6	>50
40	3,4-OMe	3,4-OMe	4.5	8.5	3.5	3.0	13.5	9.7
41	3,4-OMe	3,5-OMe	2.5	5.1	3.0	2.6	3.9	6.5
42	3,4-OMe	3,4,5-OMe	1.8	2.9	1.7	1.1	1.6	5.8
43	3,4-OMe	3-Cl-4-OH	7.1	>20	8.0	7.6	12.3	21.9
44	3,4-OMe	4-OH-3-OMe	4.5	10.3	4.6	4.6	7.9	13.7
45	3,4-OMe	3,4-OH	10.5	>20	12.1	4.2	14.4	25.2

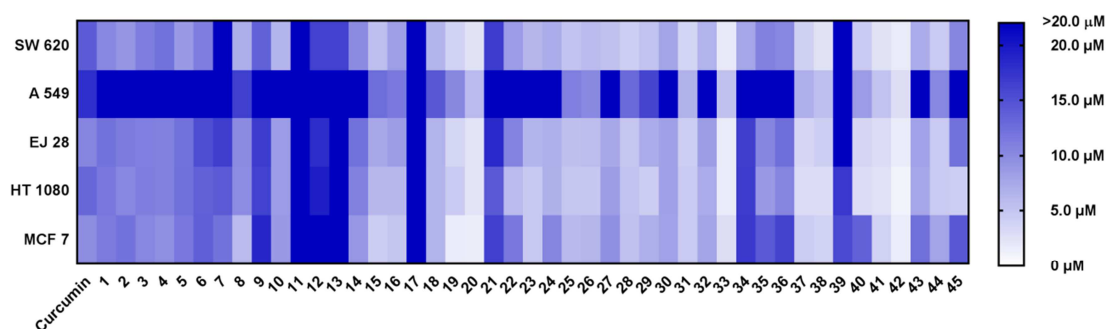


Figure 2. Overall IC_{50} distribution of compounds **1-45** against SW620, A549, EJ28, HT1080 and MCF-7

As shown in both **Table 1** and heatmap (**Figure 2**), three compounds (**20**, **33** and **42**) were found to exhibit excellent cytotoxicity in which compounds **33** and **42** were identified as the most promising candidates due to their lowest overall IC_{50} values. Meanwhile, six (**19**, **31**, **37**, **38**, **40** and **41**) and sixteen (**8**, **10**, **15**, **16**, **18**, **23**, **24**, **25**, **26**, **27**, **28**, **29**, **30**, **32**, **43** and **44**) other analogs have displayed strong and moderate cytotoxic activity with overall IC_{50} values ranging from approximately 3.0 to 5.0 μ M and 5.1 to 10 μ M, respectively. These results suggest that *meta*-substitution of phenyl ring is important for cytotoxic effect as all of the *meta*-substituted compounds possessed improved activity compared to their respective *ortho*- and *para*-substituted analogs, regardless to the substituting functional groups. This trend is clearly demonstrated in the comparisons of compounds **1-11** and **24-34** in which compounds **2**, **5**, **8**, **10**, **25**, **28**, **31** and **33** performed better in reducing cancer cells viability. On top of this, the enhanced killing effects of di-

meta substituted diarylpentanoids including **15**, **19**, **20**, **38**, **41** and **42** further confirmed the positive contribution of *meta*-substitution in anti-cancer activity.

In addition to substitution position, substituting functional group was also found to play a role in altering the cytotoxicity of synthesized compounds. According to the IC_{50} values, halogen group appeared to be essential for better cytotoxicity as brominated and chlorinated compounds including **1**, **3**, **4**, **6**, **24**, **26**, **27** and **29** shows higher inhibition than their respective methoxylated (**7**, **9**, **30**, **32**) and hydroxylated (**11** and **34**) compounds. However, this trend is only applicable to *ortho* and *para*- substitutions. The trend was completely reversed when only *meta*-substituted diarylpentanoids were being considered. As showed by compound **25** and **28**, halogenated analogs displayed much lower activity than their respective methoxylated (**31**) and hydroxylated (**33**) analogs, of which compound **33** achieved the strongest cytotoxicity with its lowest IC_{50} values ranging from 1.7 – 4.3 μ M. Similar observations found in the comparisons of compounds **2**, **5**, **8** and **10** further strengthen the reversed trend of *meta*-substituted diarylpentanoids. All these results infer that *meta*-oxygenated phenyl ring is the most crucial functionality that provides diarylpentanoid with excellent cytotoxic effects. Interestingly, compound **33** with only one *meta*-hydroxy moiety was found to exhibit similar activity to poly-methoxylated analog **42**, which implied that *meta*-hydroxylation could be a better option in preparing potent anti-cancer diarylpentanoids. In the view of their promising cytotoxicity, compounds **33** and **42** were further analyzed to evaluate and compare their anti-cancer potential.

2.2.2 Colony formation inhibition assay

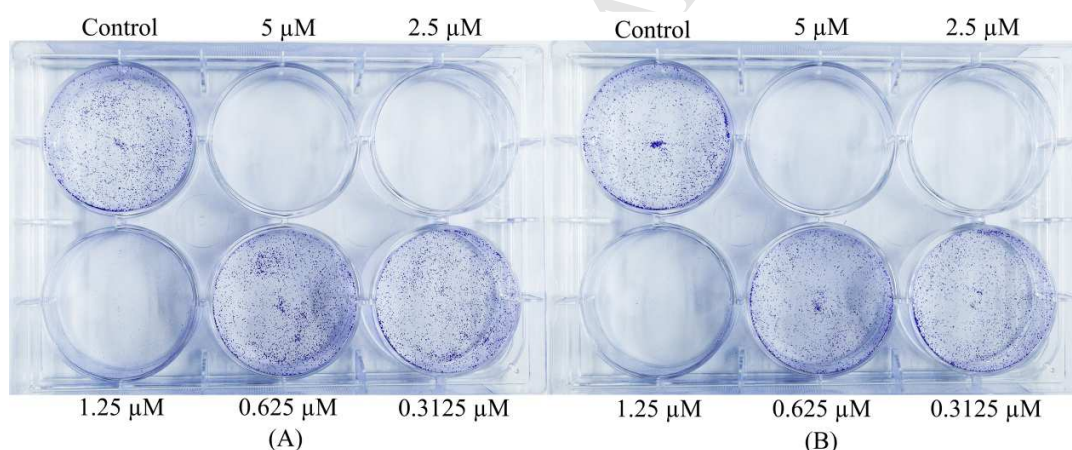


Figure 3. Representative images of SW620 cells colonies after treatment with various concentrations of compounds **33** (A) and **42** (B) for 10 days

Colony formation assay on colorectal cancer cell line (SW620) was employed to evaluate the anti-proliferative properties of compound **33** and **42**. As showed in **Figure 3A**, no colonies were observed in the cells treated with 2.5 and 5 μ M of compounds **33**. Meanwhile, only few colonies were formed in the cells treated with 1.25 μ M of the same compound. Similar observations were also made in cells treated with compound **42** (**Figure 3B**). These results suggest that both compounds **33** and **42** are strong anti-proliferative agents. Further quantification using ImegeJ software revealed that compound **42** performed slightly better than compound **33** based on its relatively lower percentage of colony formation at the concentration of 0.625 μ M [37]. The quantified results were plotted into a bar graph as shown in **Figure 4**.

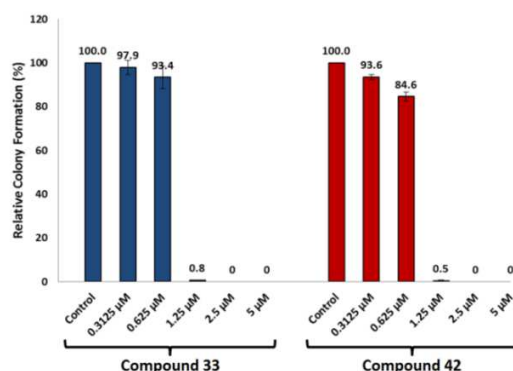


Figure 4. Relative colony formation of SW620 cells after 10 days of treatments with selected compounds at various concentrations. Blue and red bars represent the effects of compounds **33** and **42** on SW620 cell colonies, respectively.

Since anti-proliferative activity may be due to cell cycle arrest and/or cell apoptosis, we further carried out both analyses using flow cytometry to examine the possible anti-proliferative mechanism of compound **33** and **42**.

2.2.3 Cell cycle analysis

Cell cycle analyses were performed using a NovoCyte flow cytometer (ACEA Biosciences, Inc., San Diego, CA, USA). **Figure 5A** illustrates the representative cell cycle histograms of treated and untreated SW620 cells while **Figure 5B** represents the line graph plotted based on the data obtained from the flow cytometry experiments.

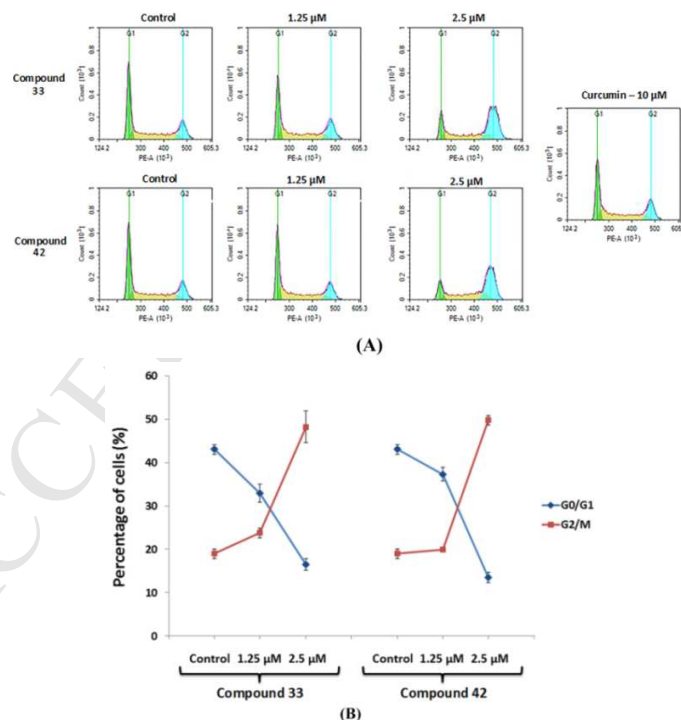


Figure 5. Representative profiles (A) and quantified data (B) of cell cycle analysis on SW620 after 24 h of treatment with various concentrations of compounds **33** and **42**. Green and blue peaks in 5A represent G1 and G2 checkpoints, respectively, while blue and red lines in 5B represent percentage of cells arrested in G0/G1 and G2/M phases, respectively.

As depicted in **Figure 5A** and **Figure 5B**, 1.25 μM of compound **33** and **42** were found to slightly increase the percentage of cells in G2/M phase from 19% to 24% and 20%, respectively. The percentages of G2/M-phase cells were further increased to 49% and 50%, respectively when 2.5 μM of same compounds were used. In contrast, the number of cells in G0/G1 phase was found to be inversely proportional to the concentration of compounds **33** and **42** as the increase in their concentrations reduced the percentage of G0/G1-arrested cells. All these results indicate that both compounds **33** and **42** could induce G2/M arrest in colorectal cancer cell line SW620.

2.2.4 Cell apoptosis study

Flow cytometry-based apoptosis analysis was carried out on SW620 cell line using Annexin V and 7-AAD double staining method (BD Biosciences, SanJose, CA, USA). **Figure 6A** and **Figure 6B** represent the dot plot diagrams resulted from the apoptosis assay using compound **33** and **42**, respectively, while the data obtained were summarized and compiled into bar graph as shown in **Figure 6C**.

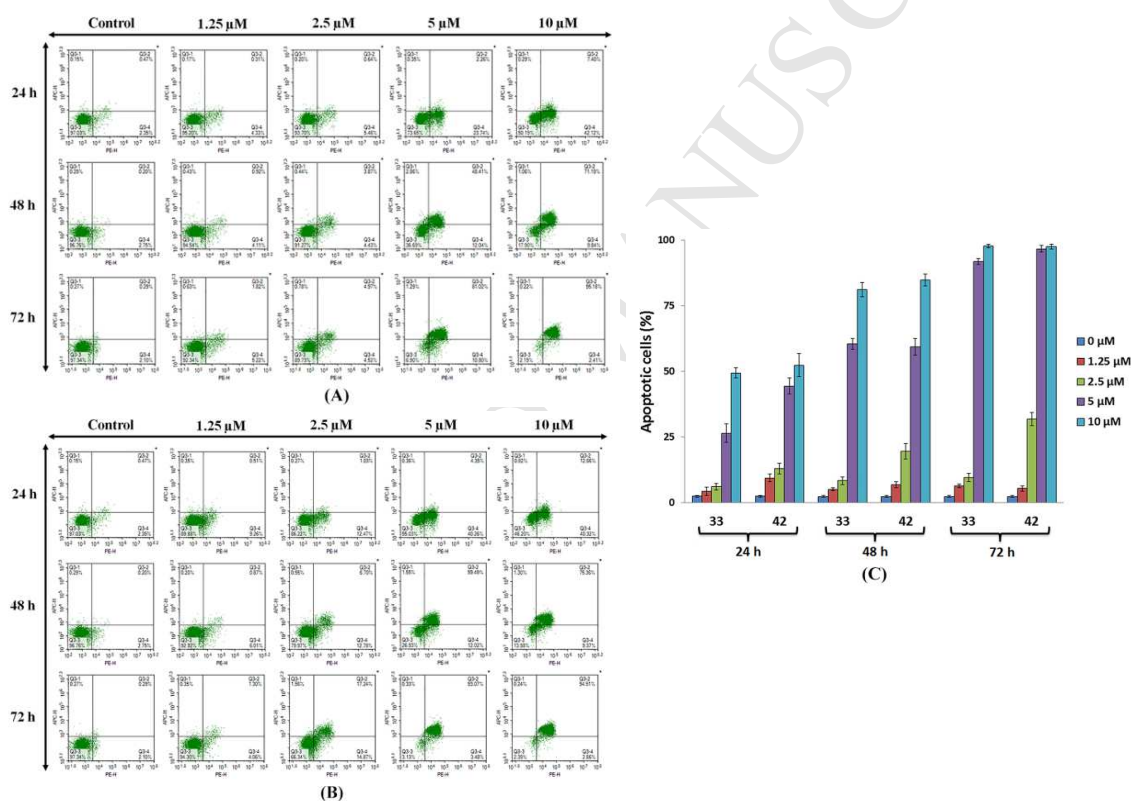


Figure 6. (A) Apoptosis profiles of SW620 treated with compound **33** at 24, 48 and 72h. (B) Apoptosis profiles of SW620 treated with compound **42** at 24, 48 and 72h. (C) Comparison of total apoptotic cells induced by compound **33** and **42** at 24, 48 and 72h.

As shown in **Figure 6A**, the treatment with 1.25 μM of compound **33** was found to barely shift the dots distribution to the right. This indicates that low dosage of compound **33** could only induce mild elevation of apoptotic cells number. However, when higher dosage of the same compound was used, the green dots that represent fluorescent cells were shifted further right reflecting an increment in the number of apoptotic cells. This dose-dependent response was also observed in cells treated with compound **42** (**Figure 6B**), whereby the increase in treatment concentrations of compound **42** has induced higher levels of cell apoptosis. Although the dot plot patterns obtained for both compounds seemed to be identical, further bar chart

comparison (**Figure 6C**) shows that compound **42** possessed a slightly stronger apoptosis inducing ability based on the higher number of apoptotic cells.

2.2.5 Intracellular reactive oxygen species (ROS) detection assay

Previous studies reported that the cell cycle arrest and cell apoptosis in response to drug treatment could be caused by the stimulation of intracellular ROS [38]. Therefore, we further explored the ability of compounds **33** and **42** in triggering the production of intracellular ROS using 2',7'-dichlorofluorescein-diacetate (DCFDA) method. DCFDA is a non-fluorescent ROS-sensitive chemical which can be easily absorbed by cells. Upon the exposure to ROS, the uptaken DCFDA will be converted into its respective highly fluorescent derivative namely 2',7'-dichlorodihydrofluorescein (DCF), and thereby causes the cells to be fluorescent. On the basis of this, the production degree of triggered ROS at different treatment concentrations can be distinguished by measuring the fluorescence intensity of treated cells. **Figure 7A** and **Figure 7B** represent the flow cytometry-based ROS profiles of cells treated with compounds **33** and **42**, respectively, while the peaks observed are corresponding to the cells with different fluorescence intensities.

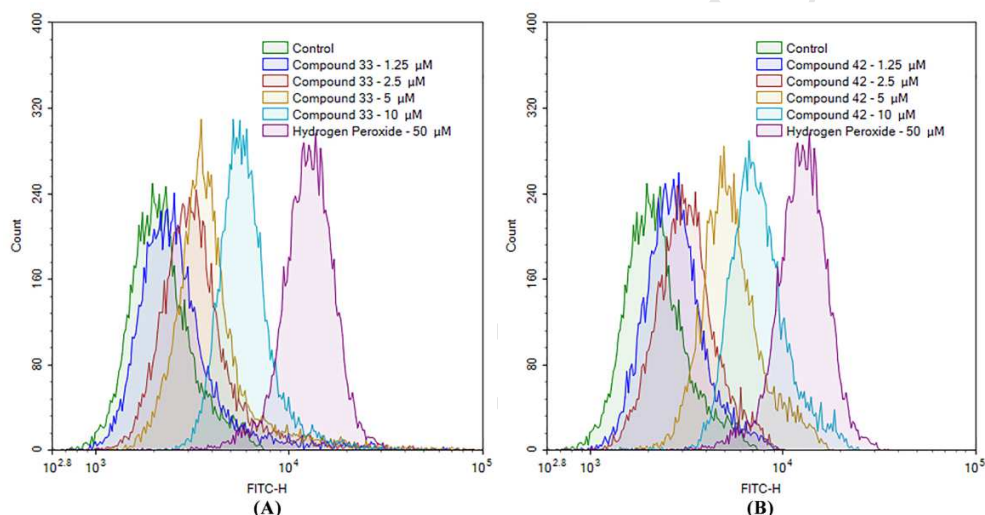


Figure 7. Representative flow cytometry-based ROS profiles of SW620 cells after treated with compounds **33** (**A**) and **42** (**B**) for 12 h.

As shown in **Figure 7**, the peak responsible for the detection of untreated cells is located at the most left region while the peak that corresponds to hydrogen peroxide treated cells is observed at the most right region. The shift from left to right indicates an increment in cellular fluorescence intensity. Interestingly, the fluorescence intensities of the treated cells were found to be directly proportional to the concentrations of compounds **33** and **42**, implying that both compounds were able to trigger the production of intracellular ROS in dose-dependent manners. Similar to previous analyses, compound **42** appeared to be a slightly better candidate based on its barely stronger intracellular ROS inducing ability.

3. Conclusion

In summary, 45 analogs of asymmetrical *meta*-methoxyphenyl-containing diarylpentanoid have been synthesized, characterized and evaluated for their anti-cancer potential against five human cancer cell lines including SW620, A549, EJ28, HT1080 and MCF-7. Compounds **33** and **42** appeared to be the most active analogs based on the determined IC_{50} values. The overall result suggested that *meta*-oxygenated phenyl ring is crucial for cytotoxicity. Subsequent colony formation assay showed that compounds **33** and **42**

possess strong anti-proliferative activity. Meanwhile, further flow cytometry experiments proved that both compounds could induce G2/M phase arrest and apoptosis in cancer cells via intracellular ROS stimulation. These results suggest that both compounds **33** and **42** are potentially to be served as antimitotic agents. Although the overall result shows that compound **42** is slightly better than compound **33**, the anti-cancer potential of *meta*-hydroxyphenyl should not be underestimated as compounds with single *meta*-hydroxylation (**33**) have displayed comparable activities to that of di-*meta*-methoxylated analogs (**41** and **42**). In conclusion, we believe that the asymmetrical diarylpentanoid system with poly *meta*-oxygenated functional groups is a promising class of natural product-based derivatives, which deserve further investigation in the development of small molecule-based anti-cancer drug.

4. Experimental Section

4.1 Chemistry

Starting materials and chemical reagents were purchased from Sigma-Aldrich and Merck, and were used without purification. Solvents were purchased from common commercial suppliers, were dried and distilled before use. The chemical reactions were routinely checked on 0.20 mm Merck TLC plate silica gel 60 F254 in every reaction step. Purification procedures were conducted using column chromatography on Merck silica gel 60 (mesh 70-230). Melting points were determined using Fisher-Johns melting point apparatus and were uncorrected. High-resolution electron ionization-mass spectrometry (HREI-MS) was determined using a DFS high resolution GC/MS (Thermo Scientific, San Jose, CA, USA). Nuclear Magnetic Resonance Spectra were recorded on Varian 500 MHz NMR Spectrometer.

4.1.1 General procedure for synthesis of **I** and **II**

Catalytic amount of *p*-toluenesulphonic acid was added into a mixture of cyclohexanone (20 mmol) and morpholine (20 mmol) in 30 mL of toluene kept in 100 mL SNRB at room temperature. The mixture was refluxed on a Dean & Stark apparatus for 2 h to obtain intermediate **I**. Upon completion, 20 mmol of 2,3- or 3,4-dimethoxybenzaldehyde in 20 mL of toluene was added dropwise into the reaction solution and heated at 80°C for 8 h. Distilled water (10 ml) was then added and further refluxed for 30 min. The resulting reaction mixture was extracted thrice with 3M HCl and once with 20 mL water. The toluene layer was then dry over anhydrous magnesium sulphate and concentrated *in vacuo* followed by purification using column chromatography to give pure 2-benzylidenecyclohexanone analog, the crucial intermediate **II**.

4.1.2 General procedure for synthesis of compound 1-45

2-Benzylidenecyclohexanone **II** (5 mmol) and appropriate aromatic aldehydes (5 mmol) were dissolved in 30 mL of absolute ethanol in a 50 mL SNRB. Catalytic amount of 6M NaOH solution was then added and stirred overnight. Subsequently, the resulting mixture was neutralized with 3M HCl followed by extraction with ethyl acetate. The organic layer was then collected and dried over anhydrous magnesium sulfate followed by evaporation with rotatory evaporator to give the crude of desired compounds. The pure asymmetrical diarylpentanoids were finally obtained through column chromatography purification.

2-(2-Chlorobenzylidene)-6-(2,3-dimethoxybenzylidene)cyclohexanone (1). Yellow viscous oil; yield: 76.21%; m.p.: -°C; Mass calculated: 368.8533; Mass found: 368.8547. ¹H NMR (500 MHz, CDCl₃) δ: 1.74 (dt, *J*=12.36, 6.33 Hz, 2 H) 2.74 - 2.78 (m, 2 H) 2.79 - 2.83 (m, 2 H) 3.83 (s, 3 H) 3.88 (s, 3 H) 6.93 (d, *J*=7.94 Hz, 2 H) 7.04 - 7.09 (m, 1 H) 7.25 - 7.29 (m, 2 H) 7.31 - 7.35 (m, 1 H) 7.41 - 7.45 (m, 1 H) 7.89 (s, 1 H) 7.95 (s, 1 H). ¹³C NMR (126 MHz, CDCl₃) δ: 23.2, 28.4, 28.7, 55.8, 61.2, 112.8, 122.1, 123.5, 126.2, 129.5, 129.7, 130.3, 130.5, 133.0, 133.6, 134.5, 135.0, 137.3, 138.0, 148.3, 152.8, 190.6

2-(3-Chlorobenzylidene)-6-(2,3-dimethoxybenzylidene)cyclohexanone (2). Yellow viscous oil; yield: 65.81%; m.p.: -; Mass calculated: 368.8533; Mass found: 368.8541. ¹H NMR (500 MHz, CDCl₃) δ: 1.8 (dt, *J*=12.67, 6.18 Hz, 2 H) 2.8 - 2.8 (m, 2 H) 2.9 - 2.9 (m, 2 H) 3.8 - 3.8 (m, 3 H) 3.9 (s, 3 H) 6.9 (d, *J*=7.94 Hz, 2 H) 7.0 - 7.1 (m, 1 H) 7.3 - 7.4 (m, 3 H) 7.4 (s, 1 H) 7.7 (s, 1 H) 7.9 (s, 1 H). ¹³C NMR (126 MHz, CDCl₃) δ: 23.0, 28.4, 28.6, 55.8, 61.1, 112.8, 122.1, 123.5, 128.4, 128.5, 129.6, 129.9, 130.2, 132.8, 134.3, 135.3, 137.2, 137.4, 137.8, 148.3, 152.8, 190.1

2-(4-Chlorobenzylidene)-6-(2,3-dimethoxybenzylidene)cyclohexanone (3). Yellow solid; yield: 85.17%; m.p.: 94-96°C; Mass calculated: 368.8533; Mass found: 368.8541. ¹H NMR (500 MHz, CDCl₃) δ: 1.8 (quin, *J*=6.26 Hz, 2 H) 2.8 - 2.8 (m, 2 H) 2.9 - 2.9 (m, 2 H) 3.8 (s, 3 H) 3.9 (s, 3 H) 6.9 (d, *J*=7.94 Hz, 2 H) 7.0 - 7.1 (m, 1 H) 7.3 - 7.4 (m, 4 H) 7.7 (s, 1 H) 7.9 (s, 1 H). ¹³C NMR (126 MHz, CDCl₃) δ: 23.1, 28.4, 28.6, 55.8, 61.1, 112.8, 122.1, 123.5, 128.6, 130.3, 131.6, 132.7, 134.4, 135.6, 137.2, 148.3, 152.8, 190.1

2-(2-Bromobenzylidene)-6-(2,3-dimethoxybenzylidene)cyclohexanone (4). Yellow viscous oil; yield: 74.22%; m.p.: -; Mass calculated: 413.3043; Mass found: 413.3068. ¹H NMR (500 MHz, CDCl₃) δ: 1.7 (dt, *J*=12.36, 6.33 Hz, 2 H) 2.7 - 2.8 (m, 2 H) 2.8 - 2.8 (m, 2 H) 3.8 (s, 3 H) 3.9 (s, 3 H) 6.9 - 7.0 (m, 2 H) 7.0 - 7.1 (m, 1 H) 7.2 - 7.2 (m, 1 H) 7.3 - 7.4 (m, 2 H) 7.6 (d, *J*=7.94 Hz, 1 H) 7.8 (s, 1 H) 8.0 (s, 1 H). ¹³C NMR (126 MHz, CDCl₃) δ: 23.2, 28.3, 28.7, 55.8, 61.2, 112.8, 122.1, 123.5, 125.1, 126.8, 129.6, 130.3, 130.5, 132.9, 133.0, 135.9, 136.4, 137.2, 137.7, 152.8, 190.0

2-(3-Bromobenzylidene)-6-(2,3-dimethoxybenzylidene)cyclohexanone (5). Yellow solid; yield: 54.28%; m.p.: 81-83°C; Mass calculated: 413.3043; Mass found: 413.3057. ¹H NMR (500 MHz, CDCl₃) δ: 1.8 (quin, *J*=6.26 Hz, 2 H) 2.8 - 2.8 (m, 2 H) 2.9 - 2.9 (m, 2 H) 3.8 (s, 3 H) 3.9 (s, 3 H) 6.9 (d, *J*=7.93 Hz, 2 H) 7.0 - 7.1 (m, 1 H) 7.2 - 7.3 (m, 1 H) 7.4 (d, *J*=7.94 Hz, 1 H) 7.5 (d, *J*=7.94 Hz, 1 H) 7.6 (s, 1 H) 7.7 (s, 1 H) 7.9 (s, 1 H). ¹³C NMR (126 MHz, CDCl₃) δ: 23.0, 28.4, 28.6, 55.8, 61.2, 112.8, 122.1, 122.4, 123.5, 128.9, 129.9, 130.2, 131.3, 132.8, 132.8, 135.2, 137.2, 137.5, 138.1, 148.3, 152.8, 190.0

2-(4-Bromobenzylidene)-6-(2,3-dimethoxybenzylidene)cyclohexanone (6). Yellow solid; yield: 77.71%; m.p.: 101-102°C; Mass calculated: 413.3043; Mass found: 413.3048. ¹H NMR (500 MHz, CDCl₃) δ: 1.8 (quin, *J*=6.26 Hz, 2 H) 2.8 - 2.8 (m, 2 H) 2.8 - 2.9 (m, 2 H) 3.8 (s, 3 H) 3.9 (s, 3 H) 6.9 (d, *J*=7.93 Hz, 2 H) 7.0 - 7.1 (m, 1 H) 7.3 (d, *J*=8.55 Hz, 2 H) 7.5 (d, *J*=8.55 Hz, 2 H) 7.7 (s, 1 H) 7.9 (s, 1 H). ¹³C NMR (126 MHz, CDCl₃) δ: 23.1, 28.4, 28.7, 55.8, 61.1, 112.8, 122.1, 122.8, 123.5, 130.3, 131.6, 131.8, 132.7, 134.9, 135.6, 136.9, 137.2, 148.3, 152.8, 190.1

2-(2,3-Dimethoxybenzylidene)-6-(2-methoxybenzylidene)cyclohexanone (7). Yellow viscous oil; yield: 43.21%; m.p.: -; Mass calculated: 364.4343; Mass found: 364.4353. ¹H NMR (500 MHz, CDCl₃) δ: 1.7 (dt, *J*=12.67, 6.18 Hz, 2 H) 2.8 (t, *J*=6.41 Hz, 2 H) 2.8 - 2.9 (m, 2 H) 3.8 (s, 3 H) 3.9 (s, 3 H) 3.9 - 3.9 (m, 3 H) 6.9 - 6.9 (m, 3 H) 7.0 (t, *J*=7.63 Hz, 1 H) 7.0 - 7.1 (m, 1 H) 7.3 - 7.4 (m, 2 H) 7.9 (s, 1 H) 8.0 (s, 1 H). ¹³C NMR (126 MHz, CDCl₃) δ: 23.4, 28.7, 28.8, 55.5, 55.8, 61.1, 110.6, 112.6, 119.9, 122.2, 123.4, 125.0, 130.1, 130.3, 132.2, 132.7, 136.4, 137.7, 148.3, 152.8, 158.4, 190.4

2-(2,3-Dimethoxybenzylidene)-6-(3-methoxybenzylidene)cyclohexanone (8). Yellow viscous oil; yield: 38.77%; m.p.: -; Mass calculated: 364.4343; Mass found: 364.4361. ¹H NMR (500 MHz, CDCl₃) δ: 1.8 (dt, *J*=12.36, 6.33 Hz, 2 H) 2.8 - 2.8 (m, 2 H) 2.9 - 2.9 (m, 2 H) 3.8 (s, 3 H) 3.8 (s, 3 H) 3.9 (s, 3 H) 6.9 - 6.9 (m, 3 H) 7.0 (s, 1 H) 7.0 - 7.1 (m, 2 H) 7.3 (t, *J*=7.94 Hz, 1 H) 7.8 (s, 1 H) 7.9 (s, 1 H). ¹³C NMR (126 MHz, CDCl₃) δ: 23.1, 28.5, 28.7, 55.3, 55.8, 61.1, 112.7, 114.2, 115.7, 122.1, 122.8, 123.5, 129.3, 130.4, 132.5, 136.6, 136.9, 137.3, 137.4, 148.3, 152.8, 159.4, 190.3

2-(2,3-Dimethoxybenzylidene)-6-(4-methoxybenzylidene)cyclohexanone (9). Yellow solid; yield: 43.15%; m.p.: 114-115°C; Mass calculated: 364.4343; Mass found: 364.4352. ¹H NMR (500 MHz, CDCl₃) δ: 1.8 (quin, *J*=6.26 Hz, 2 H) 2.8 - 2.8 (m, 2 H) 2.9 - 2.9 (m, 2 H) 3.8 (s, 3 H) 3.8 (s, 3 H) 3.9 (s, 3 H) 6.9 - 7.0 (m, 4 H) 7.0 - 7.1 (m, 1 H) 7.5 (d, *J*=8.55 Hz, 2 H) 7.8 (s, 1 H) 7.9 (s, 1 H). ¹³C NMR (126 MHz, CDCl₃) δ: 23.2, 28.4, 28.8, 55.3, 55.8, 61.1, 112.6, 113.9, 122.1, 123.4, 128.7, 130.5, 132.0, 132.3, 134.2, 137.1, 137.6, 148.2, 152.8, 160.0, 190.2

2-(2,3-Dimethoxybenzylidene)-6-(3-hydroxybenzylidene)cyclohexanone (10). Yellow solid; yield: 22.34%; m.p.: 115-117°C; Mass calculated: 350.4077; Mass found: 350.4091. ¹H NMR (500 MHz, CDCl₃) δ: 1.7 - 1.8 (m, 2 H) 2.7 - 2.8 (m, 2 H) 2.9 - 2.9 (m, 2 H) 3.8 (s, 3 H) 3.9 (s, 3 H) 6.4 (br. s., 1 H) 6.9 (dd, *J*=8.24, 2.14 Hz, 1 H) 6.9 (d, *J*=7.93 Hz, 2 H) 7.0 - 7.0 (m, 2 H) 7.0 - 7.1 (m, 1 H) 7.2 - 7.3 (m, 1 H) 7.8 (s, 1 H) 7.9 (s, 1 H). ¹³C NMR (126 MHz, CDCl₃) δ: 23.0, 28.4, 28.6, 55.9, 61.2, 110.0, 112.9, 116.1, 117.4, 122.1, 122.5, 123.5, 129.5, 130.2, 132.9, 136.4, 137.3, 137.5, 148.3, 152.8, 156.0, 191.0

2-(2,3-Dimethoxybenzylidene)-6-(4-hydroxybenzylidene)cyclohexanone (11). Yellow solid; yield: 33.82%; m.p.: 161-163°C; Mass calculated: 350.4077; Mass found: 350.4084. ¹H NMR (500 MHz, acetone) δ: 1.8 (quin, *J*=6.36 Hz, 2 H) 2.8 - 2.8 (m, 2 H) 2.9 - 3.0 (m, 2 H) 3.8 (s, 3 H) 3.9 (s, 3 H) 6.9 (d, *J*=8.67 Hz, 2 H) 7.0 - 7.0 (m, 1 H) 7.0 - 7.1 (m, 2 H) 7.5 (d, *J*=8.67 Hz, 2 H) 7.7 (s, 1 H) 7.9 (s, 1 H) 8.8 (s, 1 H). ¹³C NMR (126 MHz, acetone) δ: 23.0, 28.1, 28.5, 55.3, 60.0, 113.2, 115.5, 121.8, 123.5, 130.2, 130.8, 132.5, 133.7, 136.5, 137.3, 148.4, 153.0, 158.3, 188.4

2-(2,3-Dichlorobenzylidene)-6-(2,3-dimethoxybenzylidene)cyclohexanone (12). Yellow viscous oil; yield: 44.57%; m.p.: - ; Mass calculated: 403.2984; Mass found: 403.2993. ¹H NMR (500 MHz, CDCl₃) δ: 1.7 (dt, *J*=12.67, 6.18 Hz, 2 H) 2.7 - 2.7 (m, 2 H) 2.8 - 2.8 (m, 2 H) 3.8 (s, 3 H) 3.9 (s, 3 H) 6.9 (d, *J*=7.93 Hz, 2 H) 7.0 - 7.1 (m, 1 H) 7.2 - 7.2 (m, 2 H) 7.4 - 7.5 (m, 1 H) 7.8 (s, 1 H) 8.0 (s, 1 H). ¹³C NMR (126 MHz, CDCl₃) δ: 23.2, 28.4, 28.7, 55.9, 61.2, 112.9, 122.1, 123.5, 126.6, 126.7, 128.6, 130.0, 130.2, 132.3, 132.9, 133.3, 136.8, 137.1, 138.6, 148.3, 152.8, 189.9

2-(2,4-Dichlorobenzylidene)-6-(2,3-dimethoxybenzylidene)cyclohexanone (13). Yellow solid; yield: 53.14%; m.p.: 96-96°C; Mass calculated: 403.2984; Mass found: 403.2992. ¹H NMR (500 MHz, CDCl₃) δ: 1.7 (dt, *J*=12.57, 6.14 Hz, 2 H) 2.7 - 2.7 (m, 2 H) 2.8 - 2.8 (m, 2 H) 3.8 (s, 3 H) 3.9 (s, 3 H) 6.9 (d, *J*=8.09 Hz, 2 H) 7.0 - 7.1 (m, 1 H) 7.2 (s, 2 H) 7.4 (s, 1 H) 7.8 (s, 1 H) 7.9 (s, 1 H). ¹³C NMR (126 MHz, CDCl₃) δ: 23.2, 28.5, 28.6, 55.8, 61.1, 112.9, 122.1, 123.5, 126.6, 129.6, 130.2, 131.2, 132.3, 133.0, 133.2, 134.6, 135.7, 137.0, 138.5, 148.3, 152.8, 189.8

2-(3,4-Dichlorobenzylidene)-6-(2,3-dimethoxybenzylidene)cyclohexanone (14). Yellow solid; yield: 58.35%; m.p.: 105-106°C; Mass calculated: 403.2984; Mass found: 403.2989. ¹H NMR (500 MHz, CDCl₃) δ: 1.8 (dt, *J*=12.36, 6.33 Hz, 2 H) 2.8 - 2.8 (m, 2 H) 2.8 - 2.9 (m, 2 H) 3.8 (s, 3 H) 3.9 (s, 3 H) 6.9 (dd, *J*=8.24, 3.97 Hz, 2 H) 7.0 - 7.1 (m, 1 H) 7.2 - 7.3 (m, 1 H) 7.5 (d, *J*=8.55 Hz, 1 H) 7.5 (s, 1 H) 7.6 (s, 1 H) 7.9 (s, 1 H). ¹³C NMR (126 MHz, CDCl₃) δ: 23.0, 28.4, 28.6, 55.8, 61.2, 112.9, 122.1, 123.5, 129.5, 130.1, 130.4, 131.7, 132.5, 132.6, 133.0, 134.1, 136.0, 137.0, 137.8, 148.3, 152.8, 189.8

2-(3,5-Dichlorobenzylidene)-6-(2,3-dimethoxybenzylidene)cyclohexanone (15). Yellow solid; yield: 27.76%; m.p.: 136-138°C; Mass calculated: 403.2984; Mass found: 403.2997. ¹H NMR (500 MHz, CDCl₃) δ: 1.8 (dt, *J*=12.28, 6.29 Hz, 2 H) 2.8 - 2.8 (m, 2 H) 2.8 - 2.9 (m, 2 H) 3.8 (s, 3 H) 3.9 (s, 3 H) 6.9 (dd, *J*=8.09, 3.47 Hz, 2 H) 7.0 - 7.1 (m, 1 H) 7.3 - 7.3 (m, 3 H) 7.6 (s, 1 H) 7.9 (s, 1 H). ¹³C NMR (126 MHz, CDCl₃) δ: 22.9, 28.4, 28.5, 55.8, 61.1, 112.9, 122.0, 123.5, 128.2, 128.2, 133.2, 133.7, 134.9, 135.6, 135.7, 136.7, 136.9, 138.5, 138.9, 148.3, 152.8, 189.7

2,6-Bis(2,3-dimethoxybenzylidene)cyclohexanone (16). Yellow solid; yield: 69.57%; m.p.: 116-118°C; Mass calculated: 394.4602; Mass found: 394.4627. ¹H NMR (500 MHz, CDCl₃) δ: 1.7 (quin, *J*=6.26 Hz, 2 H) 2.8 (t, *J*=6.41 Hz, 4 H) 3.8 (s, 6 H) 3.9 (s, 6 H) 6.9 - 7.0 (m, 4 H) 7.0 - 7.1 (m, 2 H) 7.9 (s, 2 H). ¹³C NMR (126 MHz, CDCl₃) δ: 23.3, 28.7, 55.8, 61.1, 112.7, 122.1, 123.4, 130.4, 132.4, 137.5, 148.3, 152.8, 190.3

2-(2,3-Dimethoxybenzylidene)-6-(2,4-dimethoxybenzylidene)cyclohexanone (17). Yellow solid; yield: 43.84%; m.p.: 125-127°C; Mass calculated: 394.4602; Mass found: 394.4609. ¹H NMR (500 MHz, CDCl₃) δ: 1.7 (dt, *J*=12.28, 6.29 Hz, 2 H) 2.7 - 2.8 (m, 2 H) 2.8 - 2.9 (m, 2 H) 3.8 (s, 3 H) 3.8 (d, *J*=1.73 Hz, 6 H) 3.9 (s, 3 H) 6.5 (d, *J*=2.89 Hz, 1 H) 6.5 - 6.5 (m, 1 H) 6.9 - 6.9 (m, 2 H) 7.0 - 7.1 (m, 1 H) 7.3 (d, *J*=8.67 Hz, 1 H) 7.9 (s, 1 H) 8.0 (s, 1 H). ¹³C NMR (126 MHz, CDCl₃) δ: 23.5, 28.7, 29.0, 55.4, 55.5, 55.8, 61.1, 98.2, 104.1, 112.5, 118.0, 122.2, 123.4, 130.6, 131.2, 131.8, 132.5, 134.6, 137.8, 148.2, 152.8, 160.0, 161.6, 190.3

2-(2,3-Dimethoxybenzylidene)-6-(3,4-dimethoxybenzylidene)cyclohexanone (18). Yellow solid; yield: 60.48%; m.p.: 105-107°C; Mass calculated: 394.4602; Mass found: 394.4618. ¹H NMR (500 MHz, CDCl₃) δ: 1.8 (quin, *J*=6.18 Hz, 2 H) 2.8 - 2.8 (m, 2 H) 2.9 - 3.0 (m, 2 H) 3.8 (s, 3 H) 3.9 (s, 3 H) 3.9 (s, 3 H) 3.9 (s, 3 H) 6.9 - 6.9 (m, 3 H) 7.0 (s, 1 H) 7.0 - 7.1 (m, 1 H) 7.1 (d, *J*=8.78 Hz, 1 H) 7.8 (s, 1 H) 7.9 (s, 1 H). ¹³C NMR (126 MHz, CDCl₃) δ: 23.2, 28.4, 28.8, 55.8, 55.9, 55.9, 61.1, 110.8, 112.6, 113.7, 122.1, 123.4, 124.0, 129.0, 130.5, 132.1, 134.5, 137.3, 137.5, 148.2, 148.6, 149.6, 152.8, 190.1

2-(2,3-Dimethoxybenzylidene)-6-(3,5-dimethoxybenzylidene)cyclohexanone (19). Yellow solid; yield: 43.32%; m.p.: 85-87°C; Mass calculated: 394.4602; Mass found: 394.4618. ¹H NMR (500 MHz, CDCl₃) δ: 1.7 (dt, *J*=12.28, 6.29 Hz, 2 H) 2.7 - 2.8 (m, 2 H) 2.9 - 2.9 (m, 2 H) 3.8 (s, 9 H) 3.9 - 3.9 (m, 3 H) 6.4 (t, *J*=2.31 Hz, 1 H) 6.6 (d, *J*=2.31 Hz, 2 H) 6.9 (d, *J*=8.09 Hz, 2 H) 7.0 - 7.1 (m, 1 H) 7.7 (s, 1 H) 7.9 (s, 1 H). ¹³C NMR (126 MHz, CDCl₃) δ: 23.1, 28.5, 28.7, 55.4, 55.8, 61.1, 100.7, 108.3, 112.7, 122.1, 123.4, 130.3, 132.5, 136.7, 136.9, 137.4, 137.8, 144.1, 148.3, 152.8, 160.5, 190.3

2-(2,3-Dimethoxybenzylidene)-6-(3,4,5-trimethoxybenzylidene)cyclohexanone (20). Yellow solid; yield: 41.98%; m.p.: 141-143°C; Mass calculated: 424.4862; Mass found: 424.4871. ¹H NMR (500 MHz, CDCl₃) δ: 1.8 (quin, *J*=6.18 Hz, 2 H) 2.8 - 2.8 (m, 2 H) 2.9 - 3.0 (m, 2 H) 3.8 (s, 3 H) 3.9 (s, 12 H) 6.7 (s, 2 H) 6.9 (d, *J*=7.68 Hz, 2 H) 7.0 - 7.1 (m, 1 H) 7.7 - 7.7 (m, 1 H) 7.9 (s, 1 H). ¹³C NMR (126 MHz, CDCl₃) δ: 23.2, 28.4, 28.7, 55.8, 56.2, 61.0, 61.1, 107.8, 112.7, 122.1, 123.5, 130.4, 131.5, 132.4, 135.6, 137.2, 137.4, 148.3, 152.9, 153.0, 190.1

2-(3-Chloro-4-hydroxybenzylidene)-6-(2,3-dimethoxybenzylidene)cyclohexanone (21). Yellow solid; yield: 67.88%; m.p.: 98-100°C; Mass calculated: 384.8527; Mass found: 384.8539. ¹H NMR (500 MHz, acetone) δ: 1.7 - 1.8 (m, 2 H) 2.8 - 2.8 (m, 2 H) 2.9 - 3.0 (m, 2 H) 3.8 (s, 3 H) 3.9 (s, 3 H) 7.0 - 7.0 (m, 1 H) 7.0 - 7.1 (m, 3 H) 7.4 (dd, *J*=8.38, 2.02 Hz, 1 H) 7.6 (d, *J*=2.31 Hz, 1 H) 7.6 (s, 1 H) 7.9 (s, 1 H). ¹³C NMR (126 MHz, acetone) δ: 22.9, 28.1, 28.5, 55.3, 60.1, 110.0, 113.3, 116.7, 120.4, 121.8, 123.5, 128.9, 130.1, 130.7, 131.2, 131.9, 134.8, 135.2, 137.2, 148.4, 153.0, 188.4

2-(2,3-Dimethoxybenzylidene)-6-(4-hydroxy-3-methoxybenzylidene)cyclohexanone (22). Yellow solid; yield: 64.58%; m.p.: 121-123°C; Mass calculated: 380.4337; Mass found: 380.4349. ¹H NMR (500 MHz, acetone) δ: 1.8 (quin, *J*=6.36 Hz, 2 H) 2.8 - 2.8 (m, 2 H) 2.9 - 3.0 (m, 2 H) 3.8 (s, 3 H) 3.9 (s, 3 H) 3.9 (s, 3 H) 6.9 - 6.9 (m, 1 H) 7.0 - 7.0 (m, 1 H) 7.0 - 7.1 (m, 3 H) 7.2 (s, 1 H) 7.7 (s, 1 H) 7.9 (s, 1 H) 8.1 (s, 1 H). ¹³C NMR (126 MHz, acetone) δ: 23.1, 28.1, 28.5, 55.3, 55.4, 60.1, 113.2, 114.2, 115.1, 121.8, 123.5, 124.5, 127.9, 130.2, 130.8, 133.9, 135.1, 136.8, 137.4, 147.3, 147.7, 153.0, 188.4

2-(3,4-Dihydroxybenzylidene)-6-(2,3-dimethoxybenzylidene)cyclohexanone (23). Yellow solid; yield: 78.24%; m.p.: 122-124°C; Mass calculated: 366.4071; Mass found: 366.4083. ¹H NMR (500 MHz, acetone) δ: 1.8 (quin, *J*=6.21 Hz, 2 H) 2.9 - 2.9 (m, 2 H) 2.9 - 3.0 (m, 2 H) 3.9 (s, 3 H) 3.9 (s, 3 H) 6.9 - 6.9 (m, 1 H) 6.9 - 7.0 (m, 1 H) 7.0 - 7.0 (m, 1 H) 7.1 (d, *J*=1.73 Hz, 1 H) 7.1 (d, *J*=4.05 Hz, 2 H) 7.5 - 7.6 (m, 1 H) 7.6 - 7.7 (m, 1 H) 8.2 (br. s., 1 H) 8.3 (br. s., 1 H). ¹³C NMR (126 MHz, acetone) δ: 22.4, 28.3, 28.3, 55.2, 55.2, 110.0, 111.5, 114.1, 115.3, 117.4, 123.6, 123.8, 128.2, 128.9, 133.8, 134.6, 135.7, 136.2, 144.9, 149.2, 150.1, 188.3

2-(2-Chlorobenzylidene)-6-(3,4-dimethoxybenzylidene)cyclohexanone (24). Yellow solid; yield: 66.83%; m.p.: 107-109°C; Mass calculated: 368.8533; Mass found: 368.8544. ¹H NMR (500 MHz, CDCl₃) δ: 1.79 (quin, *J*=6.31 Hz, 2 H) 2.72 - 2.78 (m, 2 H) 2.92 - 2.99 (m, 2 H) 3.91 (s, 3 H) 3.92 (s, 3 H) 6.91 (d, *J*=8.23 Hz, 1 H) 7.02 (s, 1 H) 7.09 - 7.13 (m, 1 H) 7.25 - 7.28 (m, 2 H) 7.31 - 7.34 (m, 1 H) 7.42 - 7.45 (m, 1 H) 7.78 (s, 1 H) 7.88 (s, 1 H). ¹³C NMR (126 MHz, CDCl₃) δ: 23.1, 28.1, 28.7, 55.9, 55.9, 110.8, 113.7, 124.1, 126.2, 126.9, 128.8, 129.4, 129.7, 130.5, 133.2, 134.2, 134.6, 134.9, 137.8, 148.6, 149.7, 189.8

2-(3-Chlorobenzylidene)-6-(3,4-dimethoxybenzylidene)cyclohexanone (25). Yellow solid; yield: 53.77%; m.p.: 96-97°C; Mass calculated: 368.8533; Mass found: 368.8547. ¹H NMR (500 MHz, CDCl₃) δ: 1.81 (quin, *J*=6.31 Hz, 2 H) 2.86 - 2.92 (m, 2 H) 2.92 - 2.99 (m, 2 H) 3.91 (s, 3 H) 3.92 (s, 3 H) 6.91 (d, *J*=8.23 Hz, 1 H) 7.02 (s, 1 H) 7.12 (dd, *J*=8.23, 1.65 Hz, 1 H) 7.29 - 7.35 (m, 3 H) 7.42 (s, 1 H) 7.70 (s, 1 H) 7.76 (s, 1 H). ¹³C NMR (126 MHz, CDCl₃) δ: 22.9, 28.3, 28.5, 55.9, 55.9, 110.9, 113.7, 124.1, 128.4, 128.4, 128.8, 129.6, 129.8, 134.1, 134.3, 134.8, 137.4, 137.6, 137.8, 148.7, 149.8, 189.9

2-(4-Chlorobenzylidene)-6-(3,4-dimethoxybenzylidene)cyclohexanone (26). Yellow solid; yield: 81.31%; m.p.: 137-139°C; Mass calculated: 368.8533; Mass found: 368.8547. ¹H NMR (500 MHz, CDCl₃) δ: 1.81 (quin, *J*=6.31 Hz, 2 H) 2.86 - 2.90 (m, 2 H) 2.92 - 2.98 (m, 2 H) 3.91 (s, 3 H) 3.92 (s, 3 H) 6.91 (d, *J*=8.23 Hz, 1 H) 7.02 (d, *J*=1.65 Hz, 1 H) 7.11 (d, *J*=8.23 Hz, 1 H) 7.35 - 7.40 (m, 4 H) 7.72 (s, 1 H) 7.75 (s, 1 H). ¹³C NMR (126 MHz, CDCl₃) δ: 22.9, 28.3, 28.5, 55.9, 56.0, 110.9, 113.7, 124.0, 128.6, 128.8, 131.5, 134.1, 134.4, 134.5, 135.1, 136.7, 137.5, 148.6, 149.7, 189.9

2-(2-Bromobenzylidene)-6-(3,4-dimethoxybenzylidene)cyclohexanone (27). Yellow solid; yield: 64.71%; m.p.: 111-112°C; Mass calculated: 413.3043; Mass found: 413.3055. ¹H NMR (500 MHz, CDCl₃) δ: 1.8 (quin, *J*=6.21 Hz, 2 H) 2.7 - 2.8 (m, 2 H) 2.9 - 3.0 (m, 2 H) 3.9 (s, 3 H) 3.9 (s, 3 H) 6.9 (d, *J*=8.09 Hz, 1 H) 7.0 (s, 1 H) 7.1 (d, *J*=8.09 Hz, 1 H) 7.2 - 7.2 (m, 1 H) 7.3 - 7.3 (m, 2 H) 7.6 (d, *J*=8.09 Hz, 1 H) 7.8 (s, 1 H) 7.8 (s, 1 H). ¹³C NMR (126 MHz, CDCl₃) δ: 23.1, 28.0, 28.7, 55.9, 110.9, 113.8, 124.1, 125.0, 126.8, 128.9, 129.5, 130.5, 131.5, 132.9, 134.2, 135.5, 136.5, 137.8, 148.7, 149.8, 189.8

2-(3-Bromobenzylidene)-6-(3,4-dimethoxybenzylidene)cyclohexanone (28). Yellow solid; yield: 56.99%; m.p.: 183-185 °C; Mass calculated: 413.3043; Mass found: 413.3048. ¹H NMR (500 MHz, CDCl₃) δ: 1.8 (dt, *J*=12.28, 6.29 Hz, 2 H) 2.9 - 2.9 (m, 2 H) 2.9 - 3.0 (m, 2 H) 3.9 (s, 3 H) 3.9 (s, 3 H) 6.9 (d, *J*=8.09 Hz, 1 H) 7.0 (s, 1 H) 7.1 (d, *J*=8.67 Hz, 1 H) 7.2 - 7.3 (m, 1 H) 7.3 - 7.4 (m, 1 H) 7.4 - 7.5 (m, 1 H) 7.6 (s, 1 H) 7.7 (s, 1 H) 7.8 (s, 1 H). ¹³C NMR (126 MHz, CDCl₃) δ: 22.9, 28.3, 28.5, 55.9, 55.9, 110.9, 113.7, 122.4, 124.1, 128.8, 128.8, 129.9, 131.3, 132.7, 134.1, 134.7, 137.4, 137.6, 138.1, 148.6, 149.8, 189.8

2-(4-Bromobenzylidene)-6-(3,4-dimethoxybenzylidene)cyclohexanone (29). Yellow solid; yield: 78.29%; m.p.: 130-131°C; Mass calculated: 413.3043; Mass found: 413.3061. ¹H NMR (500 MHz, CDCl₃) δ: 1.8 (quin, *J*=6.36 Hz, 2 H) 2.8 - 2.9 (m, 2 H) 2.9 - 3.0 (m, 2 H) 3.9 (s, 3 H) 3.9 (s, 3 H) 6.9 (d, *J*=8.09 Hz, 1 H) 7.0 (s, 1 H) 7.1 (d, *J*=8.09 Hz, 1 H) 7.3 (d, *J*=8.09 Hz, 2 H) 7.5 (d, *J*=8.09 Hz, 2 H) 7.7 (s, 1 H) 7.7 (s,

1 H). ^{13}C NMR (126 MHz, CDCl_3) δ : 22.9, 28.3, 28.5, 55.9, 110.8, 113.7, 122.7, 124.0, 128.5, 128.8, 131.6, 131.7, 134.1, 134.9, 135.2, 136.8, 137.5, 148.6, 149.7, 189.9

2-(3,4-Dimethoxybenzylidene)-6-(2-methoxybenzylidene)cyclohexanone (30). Yellow solid; yield: 33.09%; m.p.: 125-126°C; Mass calculated: 364.4343; Mass found: 364.4355. ^1H NMR (500 MHz, CDCl_3) δ : 1.8 (quin, $J=6.18$ Hz, 2 H) 2.8 - 2.9 (m, 2 H) 2.9 - 3.0 (m, 2 H) 3.9 (s, 3 H) 3.9 (s, 3 H) 3.9 (s, 3 H) 6.9 - 6.9 (m, 2 H) 7.0 (t, $J=7.41$ Hz, 1 H) 7.0 (d, $J=2.20$ Hz, 1 H) 7.1 (dd, $J=8.23, 1.65$ Hz, 1 H) 7.3 - 7.3 (m, 2 H) 7.8 (t, $J=2.47$ Hz, 1 H) 8.0 (s, 1 H). ^{13}C NMR (126 MHz, CDCl_3) δ : 23.2, 28.4, 28.8, 55.5, 55.9, 55.9, 110.0, 110.6, 110.8, 113.7, 119.9, 123.9, 129.1, 130.0, 130.3, 132.3, 134.6, 136.3, 137.0, 148.6, 149.5, 158.3, 190.2

2-(3,4-Dimethoxybenzylidene)-6-(3-methoxybenzylidene)cyclohexanone (31). Yellow viscous oil; yield: 44.03%; m.p.: -; Mass calculated: 364.4343; Mass found: 364.4350. ^1H NMR (500 MHz, CDCl_3) δ : 1.8 (quin, $J=6.18$ Hz, 2 H) 2.9 - 3.0 (m, 4 H) 3.8 (s, 3 H) 3.9 (s, 3 H) 3.9 (s, 3 H) 6.9 - 6.9 (m, 2 H) 7.0 (s, 1 H) 7.0 (d, $J=1.65$ Hz, 1 H) 7.1 (d, $J=7.68$ Hz, 1 H) 7.1 (d, $J=8.23$ Hz, 1 H) 7.3 - 7.3 (m, 1 H) 7.8 (s, 2 H). ^{13}C NMR (126 MHz, CDCl_3) δ : 23.0, 28.4, 28.6, 55.3, 55.9, 55.9, 110.9, 113.7, 114.1, 115.7, 122.8, 124.0, 128.9, 129.3, 134.4, 136.4, 136.5, 137.2, 137.4, 148.6, 149.7, 159.4, 190.2

2-(3,4-Dimethoxybenzylidene)-6-(4-methoxybenzylidene)cyclohexanone (32). Yellow solid; yield: 51.36%; m.p.: 142-144°C; Mass calculated: 364.4343; Mass found: 364.4353. ^1H NMR (500 MHz, CDCl_3) δ : 1.8 (quin, $J=6.31$ Hz, 2 H) 2.9 - 3.0 (m, 4 H) 3.8 (s, 3 H) 3.9 (s, 3 H) 3.9 (s, 3 H) 6.9 (d, $J=8.23$ Hz, 1 H) 6.9 - 6.9 (m, 2 H) 7.0 (d, $J=2.20$ Hz, 1 H) 7.1 (dd, $J=8.78, 1.65$ Hz, 1 H) 7.4 - 7.5 (m, 2 H) 7.8 (d, $J=8.23$ Hz, 2 H). ^{13}C NMR (126 MHz, CDCl_3) δ : 23.0, 28.5, 28.5, 55.3, 55.9, 55.9, 110.8, 113.6, 113.9, 123.9, 128.7, 129.0, 132.2, 134.2, 134.6, 136.6, 136.7, 148.6, 149.5, 159.9, 190.1

2-(3,4-Dimethoxybenzylidene)-6-(3-hydroxybenzylidene)cyclohexanone (33). Yellow solid; yield: 31.84%; m.p.: 129-131°C; Mass calculated: 350.4077; Mass found: 350.4085. ^1H NMR (500 MHz, CDCl_3) δ : 1.8 (dt, $J=12.49, 6.11$ Hz, 2 H) 2.9 - 3.0 (m, 4 H) 3.9 (s, 3 H) 3.9 (s, 3 H) 6.5 (br. s., 1 H) 6.9 (dd, $J=8.23, 2.74$ Hz, 1 H) 6.9 (d, $J=8.23$ Hz, 1 H) 7.0 - 7.0 (m, 3 H) 7.1 (d, $J=8.78$ Hz, 1 H) 7.2 - 7.3 (m, 1 H) 7.7 - 7.8 (m, 2 H). ^{13}C NMR (126 MHz, CDCl_3) δ : 22.9, 28.4, 28.5, 55.9, 110.0, 110.9, 113.8, 116.0, 117.4, 122.4, 124.2, 128.8, 129.6, 134.3, 136.4, 137.3, 137.9, 148.6, 149.8, 156.0, 190.9

2-(3,4-Dimethoxybenzylidene)-6-(4-hydroxybenzylidene)cyclohexanone (34). Yellow solid; yield: 50.19%; m.p.: 146-148°C; Mass calculated: 350.4077; Mass found: 350.4083. ^1H NMR (500 MHz, acetone) δ : 1.8 (dt, $J=12.49, 6.11$ Hz, 2 H) 2.9 - 3.0 (m, 2 H) 3.0 - 3.0 (m, 2 H) 3.9 (s, 3 H) 3.9 (s, 3 H) 6.9 - 6.9 (m, 2 H) 7.0 - 7.0 (m, 1 H) 7.1 - 7.1 (m, 2 H) 7.4 (d, $J=8.78$ Hz, 2 H) 7.6 (d, $J=2.20$ Hz, 2 H) 8.8 - 8.9 (m, 1 H). ^{13}C NMR (126 MHz, acetone) δ : 22.9, 28.3, 28.3, 55.2, 55.2, 111.4, 114.1, 115.4, 123.8, 127.5, 128.8, 132.4, 133.8, 134.6, 135.8, 135.9, 149.1, 150.1, 158.2, 188.3

2-(2,3-Dichlorobenzylidene)-6-(3,4-dimethoxybenzylidene)cyclohexanone (35). Yellow solid; yield: 40.25%; m.p.: 121-122°C; Mass calculated: 403.2984; Mass found: 403.2996. ^1H NMR (500 MHz, CDCl_3) δ : 1.8 (quin, $J=6.18$ Hz, 2 H) 2.7 - 2.7 (m, 2 H) 2.9 - 3.0 (m, 2 H) 3.9 (s, 3 H) 3.9 (s, 3 H) 6.9 (d, $J=8.23$ Hz, 1 H) 7.0 (d, $J=1.65$ Hz, 1 H) 7.1 - 7.1 (m, 1 H) 7.2 - 7.2 (m, 2 H) 7.4 (dd, $J=6.59, 2.74$ Hz, 1 H) 7.8 (s, 1 H) 7.8 (s, 1 H). ^{13}C NMR (126 MHz, CDCl_3) δ : 23.0, 28.0, 28.7, 55.9, 55.9, 110.0,) 110.9, 113.7, 124.2, 126.7, 128.6, 128.7, 130.0, 132.9, 133.5, 134.0, 136.7, 136.9, 138.2, 138.6, 148.7, 189.6

2-(2,4-Dichlorobenzylidene)-6-(3,4-dimethoxybenzylidene)cyclohexanone (36). Yellow solid; yield: 48.41%; m.p.: 143-145°C; Mass calculated: 403.2984; Mass found: 403.2991. ^1H NMR (500 MHz, CDCl_3) δ : 1.8 (dt, $J=12.28, 6.29$ Hz, 2 H) 2.7 - 2.7 (m, 2 H) 2.9 - 3.0 (m, 2 H) 3.9 (s, 3 H) 3.9 (s, 3 H) 6.9 (d,

$J=8.09$ Hz, 1 H) 7.0 (d, $J=1.73$ Hz, 1 H) 7.1 - 7.1 (m, 1 H) 7.2 (s, 2 H) 7.4 (s, 1 H) 7.8 (s, 1 H) 7.8 (s, 1 H). ^{13}C NMR (126 MHz, CDCl_3) δ : 23.0, 28.1, 28.7, 55.9, 110.8, 113.7, 124.2, 126.6, 129.6, 131.2, 132.0, 133.1, 133.9, 134.6, 135.7, 137.0, 138.1, 138.5, 148.6, 149.8, 189.6

22-(3,4-Dichlorobenzylidene)-6-(3,4-dimethoxybenzylidene)cyclohexanone (37). Yellow solid; yield: 51.83%; m.p.: 115-117°C; Mass calculated: 403.2984; Mass found: 403.2991. ^1H NMR (500 MHz, CDCl_3) δ : 1.8 (quin, $J=6.31$ Hz, 2 H) 2.8 - 2.9 (m, 2 H) 2.9 - 3.0 (m, 2 H) 3.9 (s, 3 H) 3.9 (s, 3 H) 6.9 (d, $J=8.23$ Hz, 1 H) 7.0 (d, $J=1.65$ Hz, 1 H) 7.1 (d, $J=8.23$ Hz, 1 H) 7.2 - 7.3 (m, 1 H) 7.5 (d, $J=8.23$ Hz, 1 H) 7.5 (d, $J=1.65$ Hz, 1 H) 7.6 (s, 1 H) 7.8 (s, 1 H). ^{13}C NMR (126 MHz, CDCl_3) δ : 22.8, 28.3, 28.5, 55.9, 55.9, 110.9, 113.7, 124.1, 128.7, 129.5, 130.3, 131.6, 132.4, 132.6, 133.7, 133.9, 136.0, 137.7, 137.8, 148.7, 149.8, 189.6

2-(3,5-Dichlorobenzylidene)-6-(3,4-dimethoxybenzylidene)cyclohexanone (38). Yellow solid; yield: 18.05%; m.p.: 106-108°C; Mass calculated: 403.2984; Mass found: 403.2994. ^1H NMR (500 MHz, CDCl_3) δ : 1.77 - 1.84 (m, 2 H) 2.84 (t, $J=6.36$ Hz, 2 H) 2.94 (t, $J=6.65$ Hz, 2 H) 3.89 (s, 3 H) 3.90 (s, 3 H) 6.89 (d, $J=8.09$ Hz, 1 H) 7.00 (s, 1 H) 7.10 (d, $J=8.67$ Hz, 1 H) 7.21 - 7.32 (m, 3 H) 7.59 (s, 1 H) 7.74 (s, 1 H). ^{13}C NMR (126 MHz, CDCl_3) δ : 22.8, 28.2, 28.5, 55.9, 110.9, 113.7, 124.2, 125.0, 126.6, 128.2, 128.6, 133.3, 133.8, 134.9, 138.1, 138.4, 138.9, 148.7, 149.9, 189.5

2-(2,4-Dimethoxybenzylidene)-6-(3,4-dimethoxybenzylidene)cyclohexanone (39). Yellow solid; yield: 27.22%; m.p.: 145-147°C; Mass calculated: 394.4602; Mass found: 394.4627. ^1H NMR (500 MHz, CDCl_3) δ : 1.78 (dt, $J=12.72$, 6.36 Hz, 3 H) 2.81 - 2.85 (m, 2 H) 2.89 - 2.95 (m, 2 H) 3.83 (s, 2 H) 3.84 (s, 3 H) 3.90 (s, 3 H) 3.91 (s, 3 H) 6.47 (d, $J=2.89$ Hz, 1 H) 6.49 (dd, $J=8.38$, 2.60 Hz, 1 H) 6.89 (d, $J=8.67$ Hz, 1 H) 7.00 (d, $J=1.73$ Hz, 1 H) 7.09 (d, $J=8.67$ Hz, 1 H) 7.28 (d, $J=8.67$ Hz, 1 H) 7.73 (s, 1 H) 7.98 (s, 1 H). ^{13}C NMR (126 MHz, CDCl_3) δ : 22.7, 28.6, 28.7, 55.4, 55.5, 55.9, 98.2, 104.1, 110.8, 113.6, 118.0, 123.8, 129.1, 131.2, 132.1, 134.2, 134.6, 134.8, 136.6, 149.4, 159.9, 161.6, 190.2

2,6-Bis(3,4-dimethoxybenzylidene)cyclohexanone (40). Yellow solid; yield: 66.33%; m.p.: 135-137°C; Mass calculated: 394.4602; Mass found: 394.4624. ^1H NMR (500 MHz, CDCl_3) δ : 1.82 (quin, $J=6.31$ Hz, 2 H) 2.92 - 2.97 (m, 4 H) 3.91 (s, 6 H) 3.92 (s, 6 H) 6.90 (d, $J=8.23$ Hz, 2 H) 7.02 (d, $J=1.65$ Hz, 2 H) 7.11 (dd, $J=8.23$, 1.65 Hz, 2 H) 7.75 (s, 2 H). ^{13}C NMR (126 MHz, CDCl_3) δ : 23.0, 28.5, 55.9, 110.8, 113.7, 123.9, 129.0, 134.5, 136.8, 148.6, 149.6, 190.0

2-(3,4-Dimethoxybenzylidene)-6-(3,5-dimethoxybenzylidene)cyclohexanone (41). Yellow solid; yield: 29.33%; m.p.: 90-91°C; Mass calculated: 394.4602; Mass found: 394.4609. ^1H NMR (500 MHz, CDCl_3) δ : 1.78 (dt, $J=12.28$, 6.29 Hz, 2 H) 2.91 (dt, $J=11.85$, 6.21 Hz, 4 H) 3.79 (s, 6 H) 3.89 (s, 3 H) 3.90 (s, 3 H) 6.44 (s, 1 H) 6.58 (s, 2 H) 6.89 (d, $J=8.09$ Hz, 1 H) 7.00 (s, 1 H) 7.10 (d, $J=8.09$ Hz, 1 H) 7.69 (s, 1 H) 7.73 (s, 1 H). ^{13}C NMR (126 MHz, CDCl_3) δ : 22.9, 28.4, 28.6, 55.4, 55.9, 55.9, 100.6, 108.2, 110.8, 113.7, 124.0, 128.9, 136.5, 136.7, 137.3, 137.8, 148.6, 149.7, 160.5, 190.1

2-(3,4-Dimethoxybenzylidene)-6-(3,4,5-trimethoxybenzylidene)cyclohexanone (42). Yellow solid; yield: 17.94%; m.p.: 148-149°C; Mass calculated: 424.4862; Mass found: 424.4874. ^1H NMR (500 MHz, CDCl_3) δ : 1.8 (quin, $J=6.31$ Hz, 2 H) 2.9 - 3.0 (m, 4 H) 3.9 (s, 9 H) 3.9 (s, 3 H) 3.9 (s, 3 H) 6.7 (s, 2 H) 6.9 (d, $J=8.23$ Hz, 1 H) 7.0 (s, 1 H) 7.1 (dd, $J=8.51$, 1.92 Hz, 1 H) 7.7 (s, 1 H) 7.8 (s, 1 H). ^{13}C NMR (126 MHz, CDCl_3) δ : 23.0, 28.4, 28.5, 55.9, 56.2, 61.0, 107.8, 110.9, 113.7, 124.0, 128.9, 134.3, 135.5, 136.8, 137.2, 153.0, 190.0

2-(3-Chloro-4-hydroxybenzylidene)-6-(3,4-dimethoxybenzylidene)cyclohexanone (43). Yellow solid; yield: 35.54%; m.p.: 132-134°C; Mass calculated: 384.8527; Mass found: 384.8541. ^1H NMR (500 MHz,

acetone) δ : 1.8 (quin, $J=6.31$ Hz, 2 H) 2.9 - 3.0 (m, 2 H) 3.0 - 3.0 (m, 2 H) 3.9 (s, 3 H) 3.9 (s, 3 H) 7.0 - 7.0 (m, 1 H) 7.1 (d, $J=8.78$ Hz, 1 H) 7.1 - 7.2 (m, 2 H) 7.4 (dd, $J=8.78, 2.20$ Hz, 1 H) 7.6 (d, $J=2.20$ Hz, 1 H) 7.6 (s, 1 H) 7.6 - 7.7 (m, 1 H) 9.3 (br. s., 1 H). ^{13}C NMR (126 MHz, acetone) δ : 22.8, 28.2, 28.3, 55.2, 55.2, 111.4, 114.1, 116.7, 123.9, 128.7, 128.9, 130.6, 130.7, 131.8, 131.9, 134.2, 134.4, 135.3, 136.2, 149.1, 150.2, 188.2

2-(3,4-Dimethoxybenzylidene)-6-(4-hydroxy-3-methoxybenzylidene)cyclohexanone (44). Yellow solid; yield: 41.09%; m.p.: 89-91°C; Mass calculated: 380.4337; Mass found: 380.4349. ^1H NMR (500 MHz, acetone) δ : 1.8 (dt, $J=12.57, 6.14$ Hz, 2 H) 2.9 - 3.0 (m, 4 H) 3.9 (s, 3 H) 3.9 (s, 3 H) 3.9 (s, 3 H) 6.9 (d, $J=8.09$ Hz, 1 H) 7.0 - 7.0 (m, 1 H) 7.1 (d, $J=8.67$ Hz, 1 H) 7.1 - 7.2 (m, 3 H) 7.6 (s, 2 H) 8.1 (s, 1 H). ^{13}C NMR (126 MHz, acetone) δ : 22.9, 28.3, 28.3, 55.2, 55.2, 55.4, 111.5, 114.1, 114.1, 115.1, 123.8, 124.3, 128.0, 128.9, 134.0, 134.6, 135.7, 136.2, 147.3, 147.6, 149.2, 150.1, 188.3

2-(3,4-Dihydroxybenzylidene)-6-(3,4-dimethoxybenzylidene)cyclohexanone (45). Yellow solid; yield: 25.52%; m.p.: 108-110°C; Mass calculated: 366.4071; Mass found: 366.4082. ^1H NMR (500 MHz, acetone) δ : 1.8 (quin, $J=6.21$ Hz, 2 H) 2.8 - 2.9 (m, 2 H) 2.9 - 3.0 (m, 2 H) 3.8 (s, 3 H) 3.9 (s, 3 H) 6.9 - 6.9 (m, 1 H) 7.0 - 7.0 (m, 2 H) 7.0 - 7.1 (m, 1 H) 7.1 - 7.1 (m, 2 H) 7.6 (s, 1 H) 7.9 (s, 1 H). ^{13}C NMR (126 MHz, acetone) δ : 23.0, 28.1, 28.6, 55.3, 60.1, 110.0, 113.2, 115.3, 117.4, 121.8, 123.5, 123.8, 128.1, 130.2, 130.8, 133.7, 136.8, 137.3, 144.9, 146.4, 153.0, 188.4

4.2 Biology

4.2.1 Cells culture

A series of human cancer cell lines including colorectal (SW620), lung (A549), bladder (EJ28), fibroblast (HT1080) and breast (MCF-7) cancer cells were grown in Dulbecco's modified Eagle's medium (DMEM) containing 10% fetal bovine serum (FBS) and 1% penicillin/streptomycin at 37°C under 5% CO_2 while NHDF cells was cultured in DMEM with 5% FBS under the same condition. The medium was changed every two days. After reaching 80-90% confluence, cells were treated with 0.25% trypsin-EDTA for further passage.

4.2.2 MTT assay

Cells were seeded at a density of 1500-5000 cells per well in a 96 well plate depending on the doubling time and cell size. After 24 h of incubation at 37°C and 5% CO_2 atmosphere, the culture media was replaced with 100 μL of fresh media followed by the addition of test compounds (100 μL) in DMSO-containing culture media. The final concentration of DMSO in the well is 0.1%. The plate was further incubated for 72 h under the same condition. Upon completion, culture medium was removed and 100 μL of MTT (Thiazoyl blue tetrazolium bromide) solution (5 mg/mL in culture media) was added. After 4 h incubation at 37°C, the MTT solution was replaced with 100 μL of DMSO. The absorbance was measured in microtiter plate reader at 570 nm.

4.2.3 Colony formation assay

Cells were grown in a 6 well plate (1000 cells/well) in 2 mL of DMEM at 37°C and 5% CO_2 atmosphere overnight. After incubation, different concentrations of selected compound were added to the cells for ten days. The culture medium was replaced by the fresh drug containing medium every three days to keep cells growing for ten days. Upon completion, cells were washed with PBS and fixed with 4% paraformaldehyde for 15 min followed by cell staining with 0.5% (w/v) Crystal violet for 10 min. The plate

was then washed with tap water and dried at room temperature. Upon drying, the plate image was photographed [39].

4.2.4 Cell cycle analysis

Cells (2×10^5 cells/well) was seeded in a 6-well plate and allowed to adhere overnight. The seeded cells were then treated with selected compounds at different concentrations for 24 h. After treatment, the cells were harvested and washed with PBS followed by fixation with 70% ethanol for overnight at 4°C. The fixed cells were then centrifuged (1200 rpm for 5 min) and the pellet was washed twice with PBS followed by addition of DNase-free RNase A solution (1 mg/ml). After 15 min of incubation, propidium iodide staining buffer (PI; 10 mg/ml) was added and the resulting mixture was further incubated for 20 min at 4°C in the dark. Lastly, samples were analyzed for propidium iodide-DNA fluorescence from 10000 events by flow cytometry [40].

4.2.5 Cell apoptosis analysis

Cells were seeded in a 6 well plate (2×10^5 cells/well) and allowed to adhere overnight. The seeded cells were then treated with the selected compounds at different concentrations for 24, 48 and 72 h. After treatment, the cells were harvested and washed with PBS followed by the addition of $1 \times$ binding buffer (500 μ l) and Annexin V-FITC (5 μ l). The cell containing mixture was then incubated in dark at 4°C for 20 min. Prior to analysis on a flow cytometer, 5 μ l of PI was added [41].

4.2.6 Measurement of reactive oxygen species (ROS) levels

Cells were seeded in a 6 well plate (2×10^5 cells/well) and allowed to adhere overnight. The seeded cells were then treated with 10 μ M of DCFDA in culturing media for 1 h. Upon completion, the DCFDA solution was aspirated and the cells were washed with PBS for twice. Then, the cells were treated with selected compounds at different concentrations for 12 h. After treatments, resultant cells were harvested, washed and resuspended in PBS. Intensity of the formed 2',7'-dichlorofluorescein as a result of Carboxy-DCFDA hydrolysis, was finally analysed with flow-cytometer at an excitation and emission wavelength of 488 and 525 nm respectively [41].

Acknowledgments

The authors thank the Ministry of Higher Education (MOHE) of Malaysia and for financial the support under the project FRGS/1/2014/ST01/UPM/02/1 (5538011). SW. Leong is supported by the university Putra Malaysia under the post-doctoral programme.

References

- [1] J. Ferlay, I. Soerjomataram, R. Dikshit, S. Eser, C. Mathers, M. Rebelo, D.M. Parkin, D. Forman, F. Bray, Cancer incidence and mortality worldwide: sources, methods and major patterns in GLOBOCAN 2012, *Int J Cancer*, 136 (2015) E359-386.
- [2] S. McGuire, World Cancer Report 2014. Geneva, Switzerland: World Health Organization, International Agency for Research on Cancer, WHO Press, 2015, *Adv Nutr*, 7 (2016) 418-419.
- [3] S.K. Samuel, V.A. Spencer, L. Bajno, J.M. Sun, L.T. Holth, S. Oesterreich, J.R. Davie, In situ cross-linking by cisplatin of nuclear matrix-bound transcription factors to nuclear DNA of human breast cancer cells, *Cancer Res*, 58 (1998) 3004-3008.
- [4] M.A. Jordan, R.J. Toso, D. Thrower, L. Wilson, Mechanism of mitotic block and inhibition of cell proliferation by taxol at low concentrations, *Proc Natl Acad Sci U S A*, 90 (1993) 9552-9556.
- [5] D.L. Morse, H. Gray, C.M. Payne, R.J. Gillies, Docetaxel induces cell death through mitotic catastrophe in human breast cancer cells, *Mol Cancer Ther*, 4 (2005) 1495-1504.

- [6] T. Shukuya, T. Yamanaka, T. Seto, H. Daga, K. Goto, H. Saka, S. Sugawara, T. Takahashi, S. Yokota, H. Kaneda, T. Kawaguchi, S. Nagase, T. Oguri, Y. Iwamoto, T. Nishimura, Y. Hattori, K. Nakagawa, Y. Nakanishi, N. Yamamoto, G. West Japan Oncology, Nedaplatin plus docetaxel versus cisplatin plus docetaxel for advanced or relapsed squamous cell carcinoma of the lung (WJOG5208L): a randomised, open-label, phase 3 trial, *Lancet Oncol*, 16 (2015) 1630-1638.
- [7] H. Gurney, Dose calculation of anticancer drugs: a review of the current practice and introduction of an alternative, *J Clin Oncol*, 14 (1996) 2590-2611.
- [8] B.E. Bachmeier, I.V. Mohrenz, V. Mirisola, E. Schleicher, F. Romeo, C. Hohnke, M. Jochum, A.G. Nerlich, U. Pfeffer, Curcumin downregulates the inflammatory cytokines CXCL1 and -2 in breast cancer cells via NFkappaB, *Carcinogenesis*, 29 (2008) 779-789.
- [9] A. Dairam, R. Fogel, S. Daya, J.L. Limson, Antioxidant and iron-binding properties of curcumin, capsaicin, and S-allylcysteine reduce oxidative stress in rat brain homogenate, *J Agric Food Chem*, 56 (2008) 3350-3356.
- [10] M.L. Kuo, T.S. Huang, J.K. Lin, Curcumin, an antioxidant and anti-tumor promoter, induces apoptosis in human leukemia cells, *Biochim Biophys Acta*, 1317 (1996) 95-100.
- [11] R. Motterlini, R. Foresti, R. Bassi, C.J. Green, Curcumin, an antioxidant and anti-inflammatory agent, induces heme oxygenase-1 and protects endothelial cells against oxidative stress, *Free Radic Biol Med*, 28 (2000) 1303-1312.
- [12] J.L. Watson, R. Hill, P.B. Yaffe, A. Greenshields, M. Walsh, P.W. Lee, C.A. Giacomantonio, D.W. Hoskin, Curcumin causes superoxide anion production and p53-independent apoptosis in human colon cancer cells, *Cancer Lett*, 297 (2010) 1-8.
- [13] P. Anand, A.B. Kunnumakkara, R.A. Newman, B.B. Aggarwal, Bioavailability of curcumin: problems and promises, *Mol Pharm*, 4 (2007) 807-818.
- [14] V. Velaithan, K.S. Okuda, M.F. Ng, N. Samat, S.W. Leong, S.M.M. Faudzi, F. Abas, K. Shaari, S.C. Cheong, P.J. Tan, Zebrafish phenotypic screen identifies novel Notch antagonists, *Investigational new drugs*, 35 (2017) 166-179.
- [15] S.W. Leong, F. Abas, K.W. Lam, K. Shaari, N.H. Lajis, 2-Benzoyl-6-benzylidenecyclohexanone analogs as potent dual inhibitors of acetylcholinesterase and butyrylcholinesterase, *Bioorganic & medicinal chemistry*, 24 (2016) 3742-3751.
- [16] S.W. Leong, S.M. Mohd Faudzi, F. Abas, M.F. Mohd Aluwi, K. Rullah, K.W. Lam, M.N. Abdul Bahari, S. Ahmad, C.L. Tham, K. Shaari, N.H. Lajis, Nitric oxide inhibitory activity and antioxidant evaluations of 2-benzoyl-6-benzylidenecyclohexanone analogs, a novel series of curcuminoid and diarylpentanoid derivatives, *Bioorg Med Chem Lett*, 25 (2015) 3330-3337.
- [17] S.W. Leong, S.M.M. Faudzi, F. Abas, M.F.F.M. Aluwi, K. Rullah, L.K. Wai, M.N.A. Bahari, S. Ahmad, C.L. Tham, K. Shaari, Synthesis and SAR study of diarylpentanoid analogues as new anti-inflammatory agents, *Molecules*, 19 (2014) 16058-16081.
- [18] Y. Ai, B. Zhu, C. Ren, F. Kang, J. Li, Z. Huang, Y. Lai, S. Peng, K. Ding, J. Tian, Y. Zhang, Discovery of New Monocarbonyl Ligustrazine-Curcumin Hybrids for Intervention of Drug-Sensitive and Drug-Resistant Lung Cancer, *J Med Chem*, 59 (2016) 1747-1760.
- [19] W. Zhang, J. Guo, S. Li, T. Ma, D. Xu, C. Han, F. Liu, W. Yu, L. Kong, Discovery of monocarbonyl curcumin-BTP hybrids as STAT3 inhibitors for drug-sensitive and drug-resistant breast cancer therapy, *Sci Rep*, 7 (2017) 46352.
- [20] B. Liang, Z. Liu, Y. Cao, C. Zhu, Y. Zuo, L. Huang, G. Wen, N. Shang, Y. Chen, X. Yue, J. Du, B. Li, B. Zhou, X. Bu, MC37, a new mono-carbonyl curcumin analog, induces G2/M cell cycle arrest and mitochondria-mediated apoptosis in human colorectal cancer cells, *Eur J Pharmacol*, 796 (2017) 139-148.
- [21] J.L. Revalde, Y. Li, T.S. Wijeratne, P. Bugde, B.C. Hawkins, R.J. Rosengren, J.W. Paxton, Curcumin and its cyclohexanone analogue inhibited human Equilibrative nucleoside transporter 1 (ENT1) in pancreatic cancer cells, *Eur J Pharmacol*, 803 (2017) 167-173.
- [22] C. Luo, Y. Li, B. Zhou, L. Yang, H. Li, Z. Feng, Y. Li, J. Long, J. Liu, A monocarbonyl analogue of curcumin, 1,5-bis(3-hydroxyphenyl)-1,4-pentadiene-3-one (Ca 37), exhibits potent growth suppressive activity and enhances the inhibitory effect of curcumin on human prostate cancer cells, *Apoptosis*, 19 (2014) 542-553.
- [23] X. Zhang, M. Chen, P. Zou, K. Kanchana, Q. Weng, W. Chen, P. Zhong, J. Ji, H. Zhou, L. He, G. Liang, Curcumin analog WZ35 induced cell death via ROS-dependent ER stress and G2/M cell cycle arrest in human prostate cancer cells, *BMC Cancer*, 15 (2015) 866.

- [24] Y. Xia, B. Weng, Z. Wang, Y. Kang, L. Shi, G. Huang, S. Ying, X. Du, Q. Chen, R. Jin, J. Wu, G. Liang, W346 inhibits cell growth, invasion, induces cycle arrest and potentiates apoptosis in human gastric cancer cells in vitro through the NF-kappaB signaling pathway, *Tumour Biol*, 37 (2016) 4791-4801.
- [25] Q. Weng, L. Fu, G. Chen, J. Hui, J. Song, J. Feng, D. Shi, Y. Cai, J. Ji, G. Liang, Design, synthesis, and anticancer evaluation of long-chain alkoxyated mono-carbonyl analogues of curcumin, *Eur J Med Chem*, 103 (2015) 44-55.
- [26] R. Jin, Y. Xia, Q. Chen, W. Li, D. Chen, H. Ye, C. Zhao, X. Du, D. Shi, J. Wu, G. Liang, Da0324, an inhibitor of nuclear factor-kappaB activation, demonstrates selective antitumor activity on human gastric cancer cells, *Drug Des Devel Ther*, 10 (2016) 979-995.
- [27] S.W. Leong, S.M.M. Faudzi, F. Abas, M.F.F.M. Aluwi, K. Rullah, K.W. Lam, M.N.A. Bahari, S. Ahmad, C.L. Tham, K. Shaari, Nitric oxide inhibitory activity and antioxidant evaluations of 2-benzoyl-6-benzylidenecyclohexanone analogs, a novel series of curcuminoid and diarylpentanoid derivatives, *Bioorganic & medicinal chemistry letters*, 25 (2015) 3330-3337.
- [28] W. Qu, J. Xiao, H. Zhang, Q. Chen, Z. Wang, H. Shi, L. Gong, J. Chen, Y. Liu, R. Cao, J. Lv, B19, a novel monocarbonyl analogue of curcumin, induces human ovarian cancer cell apoptosis via activation of endoplasmic reticulum stress and the autophagy signaling pathway, *Int J Biol Sci*, 9 (2013) 766-777.
- [29] G. Liang, S. Yang, H. Zhou, L. Shao, K. Huang, J. Xiao, Z. Huang, X. Li, Synthesis, crystal structure and anti-inflammatory properties of curcumin analogues, *Eur J Med Chem*, 44 (2009) 915-919.
- [30] Y. Zhang, C. Zhao, W. He, Z. Wang, Q. Fang, B. Xiao, Z. Liu, G. Liang, S. Yang, Discovery and evaluation of asymmetrical monocarbonyl analogs of curcumin as anti-inflammatory agents, *Drug Des Devel Ther*, 8 (2014) 373-382.
- [31] H. Singh, M. Kumar, K. Nepali, M.K. Gupta, A.K. Saxena, S. Sharma, P.M.S. Bedi, Triazole tethered C5-curcuminoid-coumarin based molecular hybrids as novel antitubulin agents: Design, synthesis, biological investigation and docking studies, *Eur J Med Chem*, 116 (2016) 102-115.
- [32] B.F. Ruan, X. Lu, T.T. Li, J.F. Tang, Y. Wei, X.L. Wang, S.L. Zheng, R.S. Yao, H.L. Zhu, Synthesis, biological evaluation and molecular docking studies of resveratrol derivatives possessing curcumin moiety as potent antitubulin agents, *Bioorg Med Chem*, 20 (2012) 1113-1121.
- [33] G.D. Kim, J. Oh, H.J. Park, K. Bae, S.K. Lee, Magnolol inhibits angiogenesis by regulating ROS-mediated apoptosis and the PI3K/AKT/mTOR signaling pathway in mES/EB-derived endothelial-like cells, *Int J Oncol*, 43 (2013) 600-610.
- [34] T. Kaiho, K. San-Nohe, S. Kajiya, T. Suzuki, K. Otsuka, T. Ito, J. Kamiya, M. Maruyama, Cardiotonic agents. 1-Methyl-7-(4-pyridyl)-5,6,7,8-tetrahydro-3 (2H)-isoquinolinones and related compounds. Synthesis and activity, *J Med Chem*, 32 (1989) 351-357.
- [35] M.F. Mohd Aluwi, K. Rullah, B.M. Yamin, S.W. Leong, M.N. Abdul Bahari, S.J. Lim, S.M. Mohd Faudzi, J. Jalil, F. Abas, N. Mohd Fauzi, N.H. Ismail, I. Jantan, K.W. Lam, Synthesis of unsymmetrical monocarbonyl curcumin analogues with potent inhibition on prostaglandin E2 production in LPS-induced murine and human macrophages cell lines, *Bioorg Med Chem Lett*, 26 (2016) 2531-2538.
- [36] L. Lin, B. Hutzen, S. Ball, E. Foust, M. Sobo, S. Deangelis, B. Pandit, L. Friedman, C. Li, P.K. Li, J. Fuchs, J. Lin, New curcumin analogues exhibit enhanced growth-suppressive activity and inhibit AKT and signal transducer and activator of transcription 3 phosphorylation in breast and prostate cancer cells, *Cancer Sci*, 100 (2009) 1719-1727.
- [37] C.A. Schneider, W.S. Rasband, K.W. Eliceiri, NIH Image to ImageJ: 25 years of image analysis, *Nat Methods*, 9 (2012) 671-675.
- [38] J. Li, H.Y. Cheung, Z. Zhang, G.K. Chan, W.F. Fong, Andrographolide induces cell cycle arrest at G2/M phase and cell death in HepG2 cells via alteration of reactive oxygen species, *Eur J Pharmacol*, 568 (2007) 31-44.
- [39] Z.H. Li, X.Q. Liu, T.Q. Zhao, P.F. Geng, W.G. Guo, B. Yu, H.M. Liu, Design, synthesis and preliminary biological evaluation of new [1,2,3]triazolo[4,5-d]pyrimidine/thiourea hybrids as antiproliferative agents, *Eur J Med Chem*, 139 (2017) 741-749.
- [40] S.L. Chia, J. Lei, D.J. Ferguson, A. Dyer, K.D. Fisher, L.W. Seymour, Group B adenovirus enadenotucirev infects polarised colorectal cancer cells efficiently from the basolateral surface expected to be encountered during intravenous delivery to treat disseminated cancer, *Virology*, 505 (2017) 162-171.

- [41] J.B. Foo, L. Saiful Yazan, Y.S. Tor, A. Wibowo, N. Ismail, N. Armania, Y.K. Cheah, R. Abdullah, *Dillenia suffruticosa* dichloromethane root extract induced apoptosis towards MDA-MB-231 triple-negative breast cancer cells, *J Ethnopharmacol*, 187 (2016) 195-204.

ACCEPTED MANUSCRIPT

- A series of asymmetrical *meta*-methoxylated diarylpentanoids were synthesized as anti-cancer agents.
- Poly-*meta*-oxygenated analogs **33** and **42** showed potent cytotoxicity against SW620, A549, EJ28, HT1080 and MCF-7 human cancer cell lines.
- Analogs **33** and **42** showed anti-proliferative activity.
- Analogs **33** and **42** could induce intracellular ROS-mediated G2/M cell arrest and cell apoptosis.